OPEN

Characteristics of the Summating Potential Measured Across a Cochlear Implant Array as an Indicator of Cochlear Function

Jared Panario,[1] Christofer Bester,[1] Stephen John O'Leary[1,2]

Objectives: The underlying state of cochlear and neural tissue function is known to affect postoperative speech perception following cochlear implantation. The ability to assess these tissues in patients can be performed using intracochlear electrocochleography (IC ECochG). One component of ECochG is the summating potential (SP) that appears to be generated by multiple cochlear tissues. Its qualities may be able to detect the presence of functional inner hair cells, but evidence for this is limited in human cochleae. This study aimed to examine the IC SP characteristics in cochlear implantation recipients, its relationship to preoperative speech perception and audiometric thresholds, and to other IC ECochG components.

Design: This is a retrospective analysis of 113 patients' IC ECochG recordings across the array in response to a 500 Hz tone burst stimulus. Responses to condensation and rarefaction stimuli were then subtracted from one another to emphasize the cochlear microphonic and added to one another to emphasize the SP, auditory nerve neurophonic, and compound action potential. Patients were grouped based on their maximum SP deflection being large and positive (+SP), large and negative (–SP), or minimal (0 SP) to further investigate these relationships.

Results: Patients in the +SP group had better preoperative speech perception (mean consonant-vowel-consonant phoneme score 46%) compared to the –SP and 0 SP groups (consonant-vowel-consonant phoneme scores 34% and 36%, respectively, difference to +SP: $p < 0.05$). Audiometric thresholds were lowest for +SP (mean pure-tone average 50 dB HL), then –SP (65 dB HL), and highest for 0 SP patients (70 dB HL), but there was not a statistical significance between +SP and –SP groups ($p > 0.1$). There were also distinct differences between SP groups in the qualities of their other ECochG components. These included the +SP patients having larger cochlear microphonic maximum amplitude, more apical SP peak electrode locations, and a more spatially specific SP magnitude growth pattern across the array.

Conclusions: Patients with large positive SP deflection in IC ECochG have preoperatively better speech perception and lower audiometric thresholds than those without. Patterns in other ECochG components suggest its positive deflection may be an indicator of cochlear function.

Key words: Cochlear implantation, Electrocochleography, Inner hair cells, Intracochlear electrocochleography, Summating potential.

Abbreviations: a.c. = alternating current; ANSD = auditory neuropathy spectrum disorder; ANF = auditory nerve fiber/s; ANN = auditory nerve neurophonic; BM = basilar membrane; CAP = compound action potential; CF = characteristic frequency; CI = cochlear implant; CM = cochlear microphonic; CRT = cochlear response telemetry; CVC-P = consonant-vowel-consonant phoneme; d.c. = direct current; DIF = difference between alternating phase ECochG responses; EC = extracochlear; ECochG = electrocochleography; ECochG-TR = electrocochleography total response; FFT = fast Fourier transform; IC = intracochlear; IHC = inner hair cells; OHC = outer hair cells; PTA = pure-tone average; RW = round window; SP = summating potential; SRT = speech recognition threshold; SUM = addition of alternating phase ECochG responses.

(Ear & Hearing 2023;44;1088–1106)

INTRODUCTION

Intracochlear electrocochleography (IC ECochG) has the capacity to interrogate the function of residual hair cell and neural function in cochlear implant (CI) recipients. The state of preoperative cochlear and neural health is known to affect the audiological and speech perception outcomes of CI surgery (Shearer & Hansen 2019). Most patients with severe-profound sensorineural hearing loss have an unknown etiology of deafness (Blamey et al. 2013); even those with identified genetic variants are incompletely understood both in their pathophysiology and its association to ECochG response changes (Zhan et al. 2021). By utilizing IC ECochG, we may be able to better assess an individual's baseline cochlear health at the time of surgery. In turn, this could better inform our understanding of cochlear pathophysiology.

To date, IC ECochG research has mostly focused upon its utility to monitor for cochlear trauma during insertion with the intent of hearing preservation (Bester et al. 2022; Kim 2020; O'Leary et al. 2020; Trecca et al. 2020). Other applications have been studied and shown its potential to objectively assess underlying cochlear health: as a tool to define cochlear dead regions with minimal residual hair cell function (Bester et al. 2017), diagnosing auditory nerve spectrum disorder (ANSD) (Shearer et al. 2018), monitoring postoperative tissue changes in the cochlea (Dalbert et al. 2015), and informing the phenotype of genetic causes of deafness (Zhan et al. 2021). Our group has also shown that the travelling wave phenomena can be observed by recording from electrodes at multiple sites across the cochlea (Campbell et al. 2017). By using multiple electrodes along the implant array, cochlear potentials can be recorded along the cochlea from its basal to apical regions with more granularity and anatomical specificity than extracochlear (EC) recordings (Calloway et al. 2014; Campbell et al. 2015; Koka et al. 2017; Helmstaedter et al. 2018). Therefore, examination of IC ECochG recording components, especially ones that are focally generated, is likely to provide more accurate information on underlying cochlear function.

We examined four major ECochG components in response to a single-tone stimulus.

[1]Department Otolaryngology, University of Melbourne, Victoria, Australia; and [2]Royal Victorian Eye and Ear Hospital, Victoria, Australia.

Each component has contributions from multiple cochlear tissues, but most have demonstrated dominant cellular generators: (1) the cochlear microphonic (CM), an alternating current (a.c.) waveform produced primarily by transduction current through the outer hair cell (OHC) stereocilia (Dallos 1972); (2) the compound action potential (CAP) representing the synchronous auditory nerve fibers (ANF) firing at the onset of a stimulus (Eggermont 1976); (3) the auditory nerve neurophonic (ANN), another a.c. waveform, a correlate of phase-locking in ANF (Snyder & Schreiner 1984); and (4) the summating potential (SP), a sustained direct current (d.c.) deflection that follows the stimulus envelope.

The composition and cellular generators of the SP have long been contended. Some early work described three separate generators (OHC, inner hair cells [IHC], and ANF) of d.c. deflection with different amplitude and polarity qualities (Goldstein 1954). Others have contended solely OHC (Dallos & Cheatham 1976) or primarily IHC generation (Zheng et al. 1997). There may also be regional differences in the generation of the SP from basal to apical tissue of the basilar membrane (BM) (Wang et al. 2016). A recent animal study using combinations of neurotoxin (kainic acid) and an OHC-targeted toxin (kanamycin) supports the triple-generator theory (Pappa et al. 2019), with IHC the greatest generator of a positive EC-recorded SP. However, this triple-generator theory has not been demonstrated from IC ECochG recordings. Assessing the SP from an intracochlear approach should provide a closer connection between this ECochG response and local physiological function.

The tone-burst SP is a dynamic waveform, its deflection and amplitude affected by recording electrode location (Ferraro et al. 1994) and stimulus characteristics (Kupperman 1966). When ECochG responses to a single-tone stimulus are recorded at multiple points along the cochlear duct length, the amplitude of SP deflection changes and can even reverse deflection polarity (Davis et al. 1958). The largest SP amplitudes are associated with recording positions corresponding to the position of maximum amplitude of cochlear partition displacement, with polarity reversal occurring on more basally-positioned electrode recordings.

Our interest lies in examining the nature of the SP across the whole implant array, given its potential to identify focal cochlear pathology. Only one study, to our knowledge, has examined postinsertion IC SP characteristics in detail; this animal study found that whole-electrode-array IC SP measurement displays tonotopic qualities consistent with that of IHC activity (Helmstaedter et al. 2018). Whole array IC SP characteristics in human CI recipients have received limited examination in the literature. Sijgers et al. (2021) examined IC addition of alternating phase ECochG responses (SUM) traces during implant insertion in a small cohort of six patients, which may not be comparable to postinsertion recordings; regardless, no SP deflection was demonstrated. Campbell et al. (2016) presented an SP pattern across three electrodes (basal, mid, and apically positioned) in one postinsertion IC ECochG cochlea, showing IC SP deflection amplitude changed and polarity reversed across the array. Later this same group presented two single-tone stimulus whole-array SUM traces (Campbell et al. 2017). Along these arrays, only a few electrode recordings demonstrated an SP response. These corresponded with the same electrodes that recorded maximal CM and ANN responses, with no SP deflection present at any other point. Polarity reversal between electrodes was present but no clear pattern was identified. Giardina (2019) presented SUM traces recorded from the apical electrode in three human postinsertion IC ECochG recordings, but there was no clear deflection consistent with an SP demonstrated.

Here, we examined IC ECochG component characteristics across the whole implant array, using recordings from every second electrode. The analysis prioritized furthering our understanding of the IC SP and its association to preinsertion cochlear tissue health. We hypothesized that positive IC SP deflection in humans will be generated by functional IHC. Three subhypotheses were tested to this end:

1. The presence of a large, positively deflected IC-recorded SP at any point across the array will be associated with better preoperative speech perception and lower audiometric thresholds;
2. There will be differences in ECochG response patterns across the array between patients whose maximum amplitude SP deflection is large and positive compared to patients with large negative maxima; and
3. The amplitude and deflection patterns of IC positive SP deflection across the array will be consistent with the tonotopicity of IHC function.

When the SP was present, we found patterns of ECochG and preoperative hearing that indicate a large positive SP deflection may be consistent with regionally functional IHC.

MATERIALS AND METHODS

Subjects

This retrospective study used data collected from 136 ears in 132 subjects (three were bilateral) under the auspices of the Human Research and Ethics Committee of the local hospital (HREC No. 14/1171H). Only recordings of arrays with complete insertion of the array were considered. Nineteen patients were excluded because of incomplete clinical identifiers or no record of their preoperative hearing; in total 113 patients were examined. All patients were implanted with Cochlear Ltd.'s CI 422 or 522 (Sydney, Australia) implants, which use Cochlear's Slim Straight electrode array. Demographic information gathered included age at implant, gender, and etiology of hearing loss.

Recording System and Setup

Electrocochleography was recorded using the Cochlear response telemetry (CRT) system previously described (Campbell et al. 2015, 2016). Acoustic stimuli were generated digitally using a USB data acquisition card (DT9847, Data Translation, USA) and presented using an ER3A insert earphone (Etymotics, IL, USA). The acoustic stimuli were 12-msec in length with 1-msec linear onset and offset ramps, with a 50-msec interstimulus interval. Alternating rarefaction and condensation phases were presented and stored separately. The intensity of the acoustic stimuli was calibrated with peak-to-peak amplitudes equal to the dB HL scale for insert earphones (ISO 389-2:1994).

The CRT system uses the implant's Neural Response Telemetry amplifier to record from the intracochlear CI electrodes. These recordings are made between any one of the intracochlear electrodes and the extracochlear plate electrode

located on the body of the implant. Recording windows were 20-msec in duration, digitized at 20-kHz and streamed to a Dell laptop (Dell, USA), via a Cochlear Freedom programming POD. Each ECochG waveform is an average of 100 presentations. The stimuli and recording were coordinated by in-house custom-written software, which interfaced with the Freedom sound processor using the cochlear device interface libraries (4.15.02). ECochG was recorded from the most apical electrode (22) and then every second electrode until the second most basal electrode. In this study, ECochG was characterized across the electrode array in response to a 0.5-kHz tone pip, delivered at either 100-dB for patients with ≤70 dB HL at 0.5-kHz or 110-dB for those with >70 dB HL.

For all cases, the implant surgery was performed via anterior mastoidectomy and posterior tympanotomy. Round window exposure, incision, and insertion was the preferred method of array insertion. Cochleostomy and insertion via cochleostomy was performed in cases where round window (RW) insertion was not possible. Both approaches were included in this study, only two cochleostomy approaches were present in the set. All patients had their ECochG recorded immediately post complete insertion of the electrode array while the patient was still anesthetized, and closure of the wound was occurring.

ECochG Signal Analysis

Assessing Cochlear Microphonic and ANN • To estimate the CM and ANN components of the ECochG waveform, the recordings were processed by either adding the alternating phases responses (SUM) to estimate the second harmonic, which is predominantly contributed by the ANN or by subtracting them (difference between alternating phase ECochG responses [DIF]) to estimate the fundamental frequency, for which the major generator is the CM (Adunka et al. 2006; Campbell et al. 2015). Digital bandpass filtering with a 50th-order Hamming window about the 500 Hz frequency ±10% was applied to the DIF signal to isolate its fundamental component to estimate the CM. After this estimation, the magnitude of the stimulus frequency-matching CM in the DIF trace was calculated by fast Fourier transform (FFT) from the unfiltered DIF trace. For the ANN, the asymmetric neural saturating response in the SUM trace was isolated using the FFT magnitude at the second harmonic. A noise floor for each trace was calculated from FFT bins ± 2 from the frequency of interest, where each FFT bin was 62.5 Hz wide, and ECochG responses were considered robust if the amplitude exceeded the calculated noise floor plus 3 SDs. It has been established that other cochlear generators may have contributed to these responses, including neural contribution to the first harmonic in the DIF (Forgues et al. 2014) and hair distortion products contributing to the second harmonic in the SUM (Teich et al. 1989). For ease of communication, in this article, the first harmonic DIF will be referred to as CM and the second harmonic of the SUM will be referred to as ANN, although we acknowledge that other generators may contribute to these responses.

Assessing the CAP and Summating Potential • Low-frequency digital bandpass filtering between 10 and 750 Hz was used to assess the SP and CAP components within the SUM signal, also with a 50th-order Hamming window. Accurate CAP and SP measurements are less straightforward compared to the ANN and CM. In RW recordings, the CAP is present in only 50% of CI cases (Scott et al. 2016). Moreover, there is difficulty in measurement, from its highly variable morphology and latency. It also can be mixed with the ANN and SP in the SUM, and can also be evident in the DIF and interact with CM. This makes amplitude assessment not always amenable to accepted automated measurement methods (Riggs et al. 2017). Of note in this study, CAP responses to a 0.5 Hz stimulus is also of smaller amplitude compared to higher frequencies.

Although the SP can be relatively easily defined as a sustained shift in the baseline of the SUM, interpretation can be difficult. As mentioned above, the SP can be overlaid and interact with both the CAP and a.c. ECochG waveforms in the SUM response. In our experience of analyzing our ECochG data, the SP in this multiple-waveform SUM could not be confidently isolated by filtering (e.g., a Savitzky-Golay filter). We acknowledge that complex SP structure across time, with both negative and positive components within a single recording, has been documented (Kupperman 1966; Harvey & Steel 1992) but were rare in our recordings and small in amplitude (three electrode ECochG recordings in two patients). All these issues make quantification of the SP more difficult than its a.c. ECochG counterparts.

The CRT software used in IC ECochG recordings is able to capture a 20-msec duration response to a 12-msec stimulus. Due to the nature of using the implant's integrated amplifiers for recording ECochG, a negative drift was present in some recordings. Bandpass filtering around the stimulus frequency was effective at removing the drift for the assessment of the a.c. responses. However, this filtration diminished or altogether obliterated any d.c. deflection that was present in raw SUM waveforms. Due to these issues and complexities of the SUM response in our acquisition method, SP and CAP measurement were best interpreted by human observation, rather than relying on an automated measurement method.

A recent study compared visual measurement compared to an accepted automated method in RW recorded click-response SPs, which found visual SP measurement correlated better with speech scores than algorithmic measurements (Hancock et al. 2021). For all these reasons, we utilized a visual method of assessing and measuring IC CAP and SP.

Visual Measurement Method

Overview

This visual assessment method detailed below was used to capture an estimation of both the CAP and SP amplitude. This was performed in the SUM for each recorded electrode in all ears using a custom MATLAB interface designed to optimally represent the SUM for visual deflection amplitude assessment. Figures 1A–C show example DIF and SUM waveforms with filtration to illustrate a.c. waveforms, and, in the right-hand column, SUM traces filtered for d.c. deflection. These were used to measure CAP and SP amplitudes across the array. Further filtered SUM trace for SP assessment are shown in Figures 2A–F. We acknowledge that this visual method could be prone to individual assessor error and bias; therefore, we consulted extensively with our associated university statistical consulting center for guidance regarding study design and validation of this method.

CAP Approach

If visually present, the CAP was measured as the difference between visual N1 and P1 peaks. In our data set, we saw that the initial CAP waveform had occurred and its subsequent effect on deflection was minimal after 5 msec.

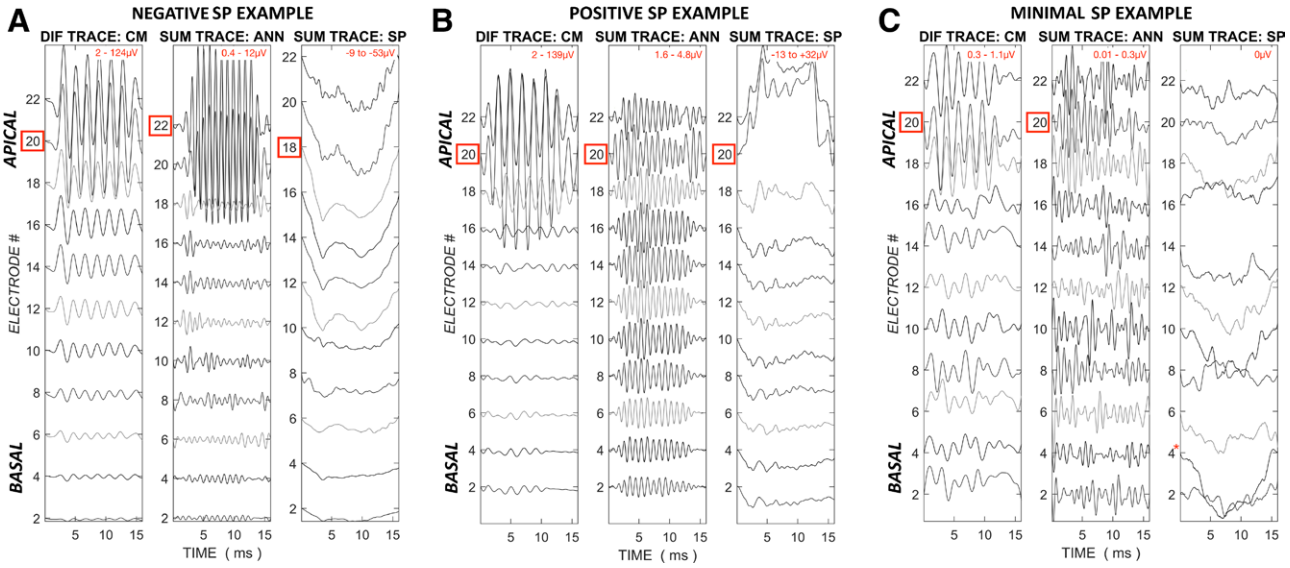

Fig. 1. Example (ECochG) recordings to a 500 Hz tone-burst stimulus across the whole implant array, from three patient cochleae. Recordings on every other electrode from base to apex. Electrode 2 is the most basal electrode recording, and electrode 22 the most apical. Scale for each trace relative to largest amplitude recording. The amplitude range for the largest response is marked in red in top right corner of each panel. The electrode at which the maximum amplitude was recorded is highlighted by a red square around the electrode number. DIF TRACE: CM shows the difference between rarefaction and condensation waveforms to highlight the cochlear microphonic (CM). SUM TRACE: ANN is the sum of rarefaction and condensation waveforms to highlight the auditory nerve neurophonic (ANN) filtered to remove drift/deflection. SUM TRACE: SP is this same SUM TRACE without this filtration to highlight the summating potential (SP) and compound action potential (CAP). A, This shows CM and ANN traces that are large and peak in the apex, accompanied by a large negative SP deflection mirroring the sound envelope that is considerably large across the apical half of the electrodes. A, CAP appears to be present in the same recordings as well, but is overlaid with the SP. B, This shows considerable amplitude CM and ANN. Compared to (A), the CM appears to be more spatially limited to the two most apical recordings and the ANN is more diffuse. The SP here shows a large positive deflection that is only present in the two most apical electrodes. There appears to be a small CAP present across all electrodes (and possibly larger in association with the large SP deflection). C, This shows small but definable CM and ANN, associated with no clear SP deflection or CAP on any recording.

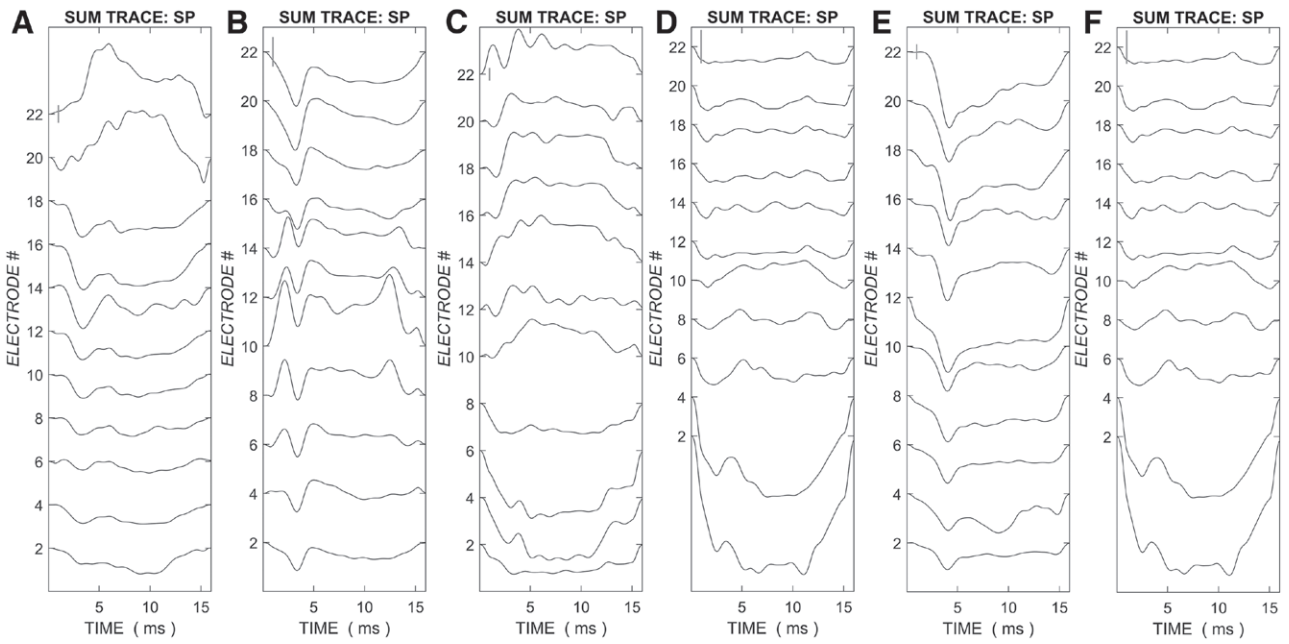

Fig. 2. Example electrocochleography (ECochG) SP SUM trace recordings to a 500 Hz tone-burst stimulus across the whole implant array, from a further six patient cochleae. Recordings on every other electrode from base to apex. Electrode 2 is the most basal electrode recording, and electrode 22 the most apical. Scale for each trace relative to largest amplitude recording, with a 10 μV scale bar (grey vertical line) placed at the beginning of electrode 22 recording for scale. Labeled (A–F) for reference. Etiology note: (A) and (B) had idiopathic sensorineural hearing loss, (C) had postinfectious hearing loss, (D) and (E) both had Ménière's disease and (F) had ANSD. A–D, Apical peak SP responses with positive (A) or negative (B–D) deflection. E, Mid array peak SP response with negative deflection. F, Basal peak SP response with negative deflection. ANSD indicates auditory neuropathy spectrum disorder; SP, summating potential.

SP Approach

The SP was measured as the deflection of the SUM trace from the baseline at the 6 to 8 msec timepoint. We had multiple reasons for electing this narrow time window: it minimized the effect of the CAP and its contribution to baseline deflection; later timepoints' reliability was limited by deflection decay from the 10 Hz low-pass filter; and it minimized the effect of the offset CAP at the end of the sound envelope. Not infrequently, a small a.c. waveform was present in the SUM at the 6 to 8 msec timepoint as a result of lighter filtration to preserve both the SP and CAP for analysis. If an a.c. potential was overlaid on a deflection in this window, the peak-trough of the a.c. waveform was measured and averaged to determine the SP. If the SP was complex (both SP+ and SP− on the same recording electrode), the SP was recorded as zero. This was rare in our data set (n = 2), and related to low amplitude responses.

Calibration and Validation

Both the CAP and SP were recorded to the nearest 1 μV, as we were interested in close estimates of amplitude rather than absolute values, acknowledging the limitations of the human eye for accurate waveform measurement. As noted earlier, the supervised SP measurement has shown better association to speech perception scores compared to automated methods. Two experienced ECochG researchers, one a clinician and the other a postdoctoral cochlear electrophysiologist, undertook the visual SP and CAP measurement method, the second assessor instructed by the first. All recordings, 1243 in total, were measured by the experienced clinician in a randomly assigned order. To demonstrate that the supervised SP from the first assessor could be replicated, 220 recordings were randomly selected to be measured by the postdoctoral electrophysiologist (measuring both CAP and SP), blind to the first set of measurements. These results were then compared using the Bland-Altman agreement method, with a cut-off of 95% of paired measurements showing <1.96 SDs of deviance to be considered valid (Bland & Altman 1986). This is an established statistical method for validating measurement approaches using the mean and difference between two independent measurements. Outliers beyond ±1.96 SD were reviewed by the two clinicians together. Agreement levels for SP and CAP measurements were 95.9% and 97.1%, respectively (Fig. 3), with most larger outliers occurring with smaller amplitude CAP and SP measurements, where the responses were harder to distinguish from noise.

A review of the discrepancies between assessors revealed that the first assessor consistently recorded 0 μV when there was doubt about the waveform's presence, while the other gave small amplitude responses in these same cases. The linear pattern of discrepancy in the CAP measurements was related to only one patient's ECochG recordings where the same difference in interpretation of small amplitude responses was found to explain the discrepancy. For this reason, smaller amplitude SP (smaller ±5 μV deflection) and CAP (under 5 μV amplitude) were considered with caution.

SP Grouping

The limitations of the visual measurement revealed three distinct groups of SP deflection that could be asserted confidently: those that were large and negative; those that were large and positive, and those that were small or absent. The assessors noted that SP deflection across the array appeared to have a peak response electrode, as has been reported previously (Campbell et al. 2017) and is consistent with the tonotopic nature of the IC SP (Helmstaedter et al. 2018). Therefore, we proposed to assess whole array recordings by separating them into three distinct groups based on their maximal SP deflection: arrays with a maximum SP that was large amplitude and positive (≥+10 μV), referred to as the +SP group; arrays with a maximum SP that was large and negative (≤−10 μV), referred to as the −SP group; and lastly those without a large SP deflection (between −10 μV and +10 μV), referred to at the 0 SP group. The latter 0 SP grouping was thought to be more reliable than attempting to differentiate between small amplitude SP or zero amplitude waveforms These amplitude limits were considered sufficiently outside of the error margin established in the Bland-Altman graph to delineate different SP response types. Cochleae with recordings that contained both large negative SP deflection in at least one electrode recording and large positive SP deflection in others were grouped based on their largest SP deflection. This group of array recordings were further assessed for the pattern of their deflection across the array.

Electrode Location Measurement • The SP, CM, and ANN all display tonotopic qualities, in part due to their generation at a localized area of the cochlea in response to a tonal stimulus. The electrode at which the maximum amplitude was measured was recorded as a variable for analysis. The recordings were from the most apical electrode (22), and then every second electrode until the second most basal electrode (2), 11 recordings in total. There were nine ears with no recordable SP deflection across the array, and 36 patients with no recordable CAP amplitude. No peak electrode was recorded in these cases of zero amplitude and patients were excluded from analysis that involved these factors. This differentiation between no recordable and small SP amplitudes is included here to display the overall pattern of deflection across the whole patient cohort. However, as noted earlier, the visual SP measurement method could not differentiate between small and zero amplitude deflection. Peak electrode locations of those cochleae with large SP deflections are assessed separately below.

Behavioral Hearing Tests

Preoperative audiometric threshold and speech perception data were obtained during implant candidacy assessment with optimized hearing aids. Only monaural scores from the ear implanted were included in the analysis. Postoperative scores were not included as part of this study as they were likely less directly correlated to preinsertional cochlear status compared to preoperative scores. Assessment of postoperative scores' relationship to postoperative outcomes is beyond the scope of our current study hypotheses and will be a focus of a separate study.

Pure-Tone Audiometry • Pure-tone audiograms were conducted in accordance with ISO 8253-1. Maximum audiometer output was 100 dB HL at 250 Hz and 120 dB HL at 500 Hz and 1 kHz. If a response was considered vibrotactile, it was considered no response. Frequencies where no behavioral responses were obtained were scored at a threshold of 120 dB HL. Puretone average (PTA) was calculated using the average of air-conduction thresholds at 250, 500, and 1000 Hz.

Speech Perception Tests • Speech perception in quiet and in noise were assessed using the consonant-vowel-consonant phoneme (CVC-P) and speech recognition threshold (SRT) scores, respectively.

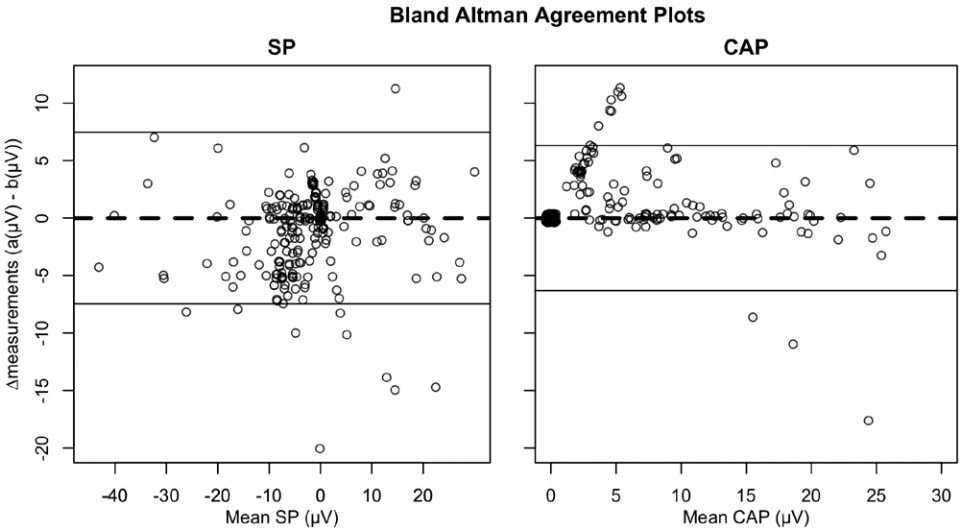

Fig. 3. Bland Altman agreement plots on the visual measurement of the summating potential (SP) and compound action potential (CAP) between two clinicians experienced in electrocochleography (ECochG). The *Y* axis is the calculated difference between the two clinicians' visual measurements (Δmeasurements), plotted against the mean of these two. The horizontal black lines are ±1.96 SDs of Δmeasurement.

Recorded open-set word and sentence materials were used for all tests using a native Australian English speaker, at 65 dB SPL at an azimuth of 0°. For CVC-P, open-set monosyllabic word testing was conducted using consonant-nucleus-consonant words spoken by a male speaker with lists of 50 words (Peterson & Lehiste 1962). CVC-P is scored as a percentage from 0% to 100% for the number of correctly identified phonemes from these lists.

Open-set sentence-in-noise testing for the SRT score was conducted using Bamford-Kowal-Bench sentence test material (Bench et al. 1979). Eighty lists of 16 simple sentences were used, with 50 key words in each list. Babble was used as the competing noise, varied for signal to noise ratios between 25 and 0 dB. SRT was measured as the average signal to noise ratio at which at least 50% of the words were repeated correctly. SRT started at 25 dB (the poorest performance score) and ended at −8 dB, although in our study group no score was <0 dB. Where CVC-P was under 10% or not recordable due to poor perception, SRT was scored at 25 dB.

Statistical Analysis and Outlier Detection

Analysis was performed using R (R Core Team, Austria) and the following packages: tidyverse (H. Wickham et al.), ggplot2 (H. Wickham, USA) and rstatix (A. Kassambara, Austria).

Data was inspected for outliers and distribution patterns. Patient and ECochG factors were plotted in box-and-whisker

TABLE 1. Demographics of study group

	Age Group			Total
	16–60 yrs	60–75 yrs	Over 75 yrs	
Number of cases	36	45	32	113
Age	47.5 (13.6)	67.4 (4.3)	79.4 (3.7)	64.6 (15)
Sex				
Male	14	22	16	52
Female	22	23	16	61
Preoperative hearing				
PTA (dB HL)	62.6 (21.6)	63.8 (19.1)	63.4 (18.9)	63.3 (19.5)
CVC-P (%)	34.5 (17.4)	37.5 (19.1)	40.2 (17.5)	37.4 (18.1)
SRT (dB)	20.1 (6.7)	20.5 (5.5)	19.3 (7.4)	19.9 (6.6)
Etiology of hearing loss				
Idiopathic SNHL	29	37	28	96
Ménière's disease	1	4	3	8
Otosclerosis		1	1	2
ANSD	2			2
Postinfectious	1 (meningitis)		1 (measles)	2
EVAS	2			2
Usher syndrome	1			1
Rhesus incompatibility		1		1
Keratitis ichthyosis		1		1
Trauma		1		1

For continuous variables, numbers are accurate to one decimal place. Number is mean value with SD in brackets.
ANSD, auditory neuropathy spectrum disorder; CVC-P, consonant-vowel-consonant phoneme; EVAS, enlarged vestibular aqueduct syndrome; PTA, pure-tone average; SNHL, sensorineural hearing loss; SRT, speech recognition threshold.

and histogram plots. These were then assessed in the context of their respective mean, interquartile ranges, and SD. Further outlier detection was done with bivariate scatterplots. Three ears had extreme bivariate outliers in maximum SP and CAP amplitudes, outside ±3 SDs from mean. Therefore, these ears were excluded. Following this, the ECochG factors were tested for interrelationships and to preoperative audiometric threshold and speech perception scores.

RESULTS

Demographics

Table 1 shows summaries of the demographic and audiological properties of the patients used in analysis. The study included more females than males (54%). There was no significant difference by gender for audiometric thresholds or speech perception ($p = 0.632$). Age ranged from 16 years to 89 years with a median age at time of operation of 69 years. There was no significant correlation of age as a continuous variable when plotted against audiometric or speech perception scores (CVC-P $r^2 = 2.5$, $p = 0.10$; SRT $r^2 = 0.98$, $p = 0.97$; PTA $r^2 = 0.09$, $p = 0.98$). If grouping by age, there was no significant difference between groups for any audiometric or speech perception outcome ($p = 0.45$).

The majority of patients hearing loss was attributed to progressive idiopathic sensorineural hearing loss (84.8%). Twenty patients had a clear etiological cause of their hearing loss, the largest associated factor was Ménière's disease, with eight patients (7.1%). Only two patients in our study had a diagnosis of ANSD.

Aside from a slightly higher percentage of female patients in the +SP group, age and gender was similar across groups (+SP 65% female, −SP 52%; average age +SP 65 years, −SP 62 years). It is interesting to note that both ANSD patients and both patients with postinfectious causes of hearing loss were in the −SP group. Ménière's disease patients were present in all groups (3 +SP patients, 2 −SP patients, and 3 0 SP patients). Preoperative hearing differences between SP groups are discussed later in this article.

ECochG Responses

Overall Trends

The histograms of the largest CM, ANN, and CAP amplitudes in each patient were strongly positively skewed, with most responses having small amplitudes (Fig. 4). Although maximum SP deflection was most often small, its histogram was instead leptokurtotic around −5 μV.

The location of all peak ECochG component responses measured across the array were biased toward the apical electrodes (Fig. 5). There were no significant differences in distribution patterns of peak locations for different ECochG components ($p = 0.86$). CAP and SP peaks were less apically skewed compared to ANN and CM peaks.

General Relationships

Amplitude and Deflection. Waveform amplitude maxima were plotted against each other in Figure 6. Linear relationships were observed between the CM, ANN, and CAP (r^2 29.3–44.3%, $p < 0.001$). Similar linear relationships existed between these waveforms and absolute SP amplitude. Deflection polarity had no apparent effect on these linear patterns, but a larger group of the −SP group had no recordable CAP. The strongest associations were between CM and ANN, and CM and SP.

Peak Electrode Position. Correlation between each ECochG component's peak position was examined using scatterplots and linear regression models. There was weak to moderate association between each ECochG response peak position. Peak position was then compared to its respective amplitude (e.g., peak CM amplitude against CM peak position). There was no significant correlation between any response's maximum amplitude and its peak electrode position (range of $r^2 = 0$–3.6%).

ECochG to Preoperative Speech Perception and Audiometric Thresholds

PTA, CVC-P, and SRT scores were correlated with peak electrode positions and maximum amplitudes by plotting the data and testing their linear association. PTA and CVC-P showed weak linear correlations to CM amplitude but no other factor (r^2 17.9% and 12.8%, respectively, both $p < 0.001$). There was no significant correlation of any ECochG factor to SRT scores.

Associations by SP Groups

Most were in the −SP and 0 SP groups (45 and 43 patients, respectively), with a smaller number in +SP group (25). Across all waveforms (SP, CM, CAP, and ANN), the maximum amplitudes differed significantly by SP grouping (Table 2 and Fig. 7). Median amplitudes tended to be higher in the +SP than the −SP groupings. This was statistically significant in post hoc pairwise analysis for the CM ($p < 0.001$), but not for absolute SP ($p = 0.11$, median +SP amplitude = 23.2 μV, −SP 17.2 μV).

Of those 25 patients within the +SP group, 12 patients (48%) also had −SP deflections ≤−10 μV within their array recordings but were smaller absolute amplitude than the +SP deflection. In the −SP group, 10 of 45 patients (22%) had +SP deflection ≥+10 μV at some point along their array recording.

Patterns of ECochG Component Amplitudes Across the Array

The amplitude of specific ECochG components, including the CM, CAP, and ANN, are presented across the length of each patient's electrode array, by first normalizing the potential against the maximum amplitude observed in each individual patient. Data from −SP and +SP groupings were presented in separate graphs (Fig. 8). Considerable interpatient variability was observed. Solid lines were passed though the median values, and for each electrode the interquartile range is overlaid. For CM, CAP, and ANN, the shape of the fitted lines was similar for both −SP and +SP groups. There did not appear to be any differences in growth patterns for CM, CAP, or ANN between the groups, but all appeared to have similar levels of growth toward the apex with minimal basal responses.

The only ECochG component that differed in amplitude growth pattern across the array was SP deflection. Some patients (n = 4) in the +SP group had points of negative deflection across the array, up to 60% magnitude of their maximum (positive) amplitude size. Some −SP patients (n = 3) had points of positive deflection somewhere on the array of up to 80% magnitude to its maximum negative deflection. The −SP best fit line suggests −SP patients' amplitude and deflection is relatively steady with little interelectrode difference, on average 40% to 50% of the maximum magnitude across the array. There was only a slight increase in relative amplitude toward the apical electrodes. In contrast, +SP groups' amplitude appears much more position dependent and tonotopic than −SP peaks. This +SP group showed exponential increase in amplitude as the toward the apex, like the other ECochG components.

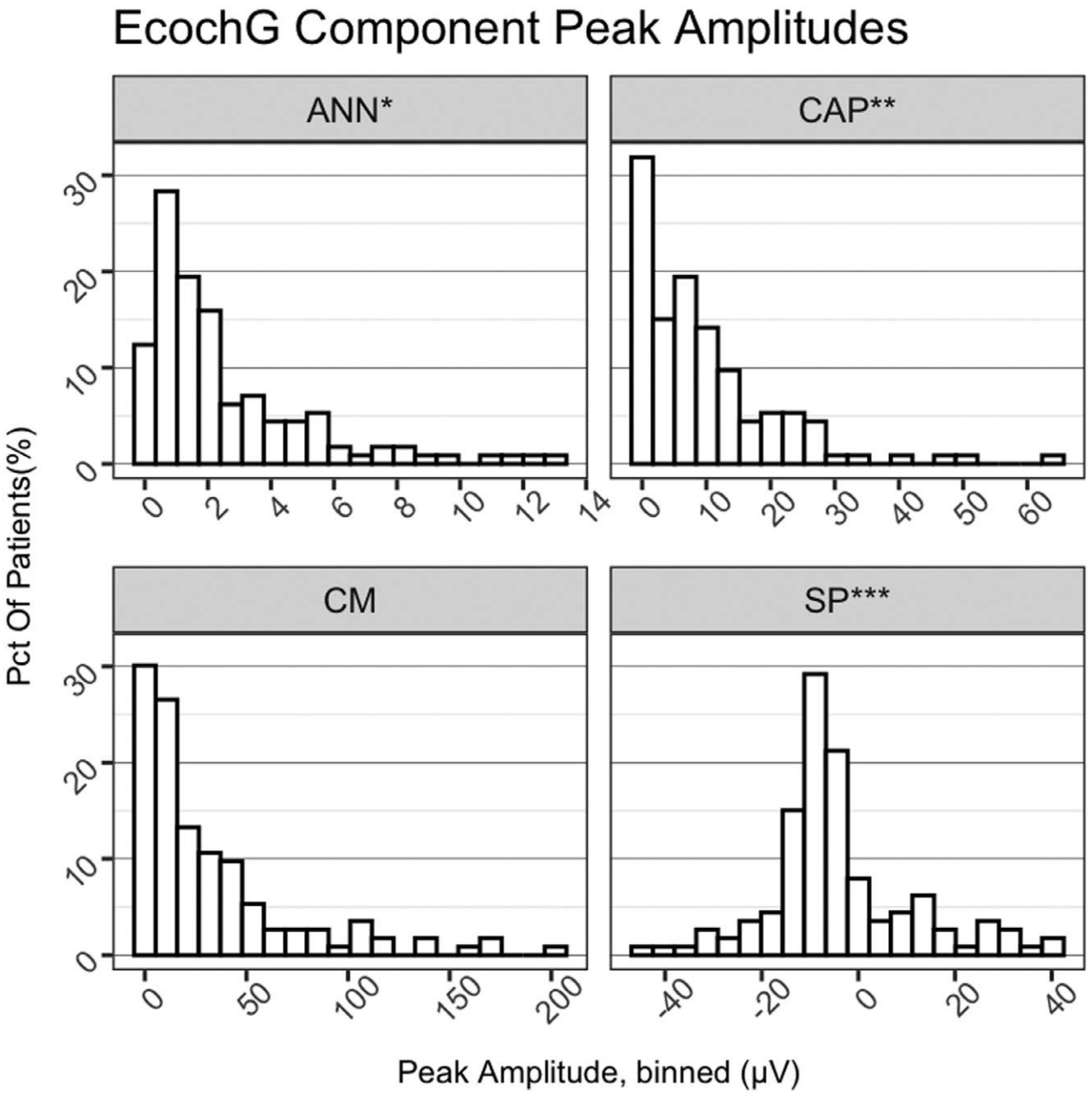

Fig. 4. A–D, Histograms of electrocochleography component peak amplitudes. Bin widths: ANN 0.76 μV, CAP 3.25 μV, CM 10 μV, and SP 4.5 μV. Outliers removed from plots to better demonstrate the bulk of the data. * ANN outliers: 3 maxima >14 μV (19.1, 21.2, and 27.3 μV). ** CAP outliers: 1 maxima > 65 μV (147 μV). *** SP outliers: 2 maxima >+45 μV (+80 and +167 μV) and one <−45 μV (−80 μV). ANN indicates auditory nerve neurophonic; CAP, compound action potential; CM, cochlear microphonic; SP, summating potential.

Patients with both positive and negative SP deflections across the array, that is, a dynamic change across the array, tended to have larger amplitude summating potentials than when a single polarity was observed. For those classified as −SP, the SP amplitude across the group was 9 μV larger when a dynamic change was observed than not (median SP amplitudes of 22 μV and 13 μV, respectively). Similarly, for +SP patients, the SP amplitude was 6 μV greater when a dynamic change was evident than not (median SP amplitudes of 26 μV and 20 μV, respectively).

Peak Locations

Electrode locations of peak ECochG components were assessed by SP group in Figure 9 and further described in Table 3. Peaks of +SP occur in four electrodes more apically than −SP peaks (+SP peak = electrode 22, −SP peak = electrode 18, Mann-Whitney U test $p = 0.023$). There was no significant distribution difference for peak locations of CM, CAP, or ANN. CAP electrode positioning appeared more apically skewed between these groups and this was not statistically significant ($p = 0.102$).

Next, the location exhibiting the peak amplitude for one waveform was plotted against the location of the peak amplitude of another waveform. The combinations examined are presented in Figure 10, considered by ±SP Grouping. For example, Figure 10A plotted the electrode on which the peak

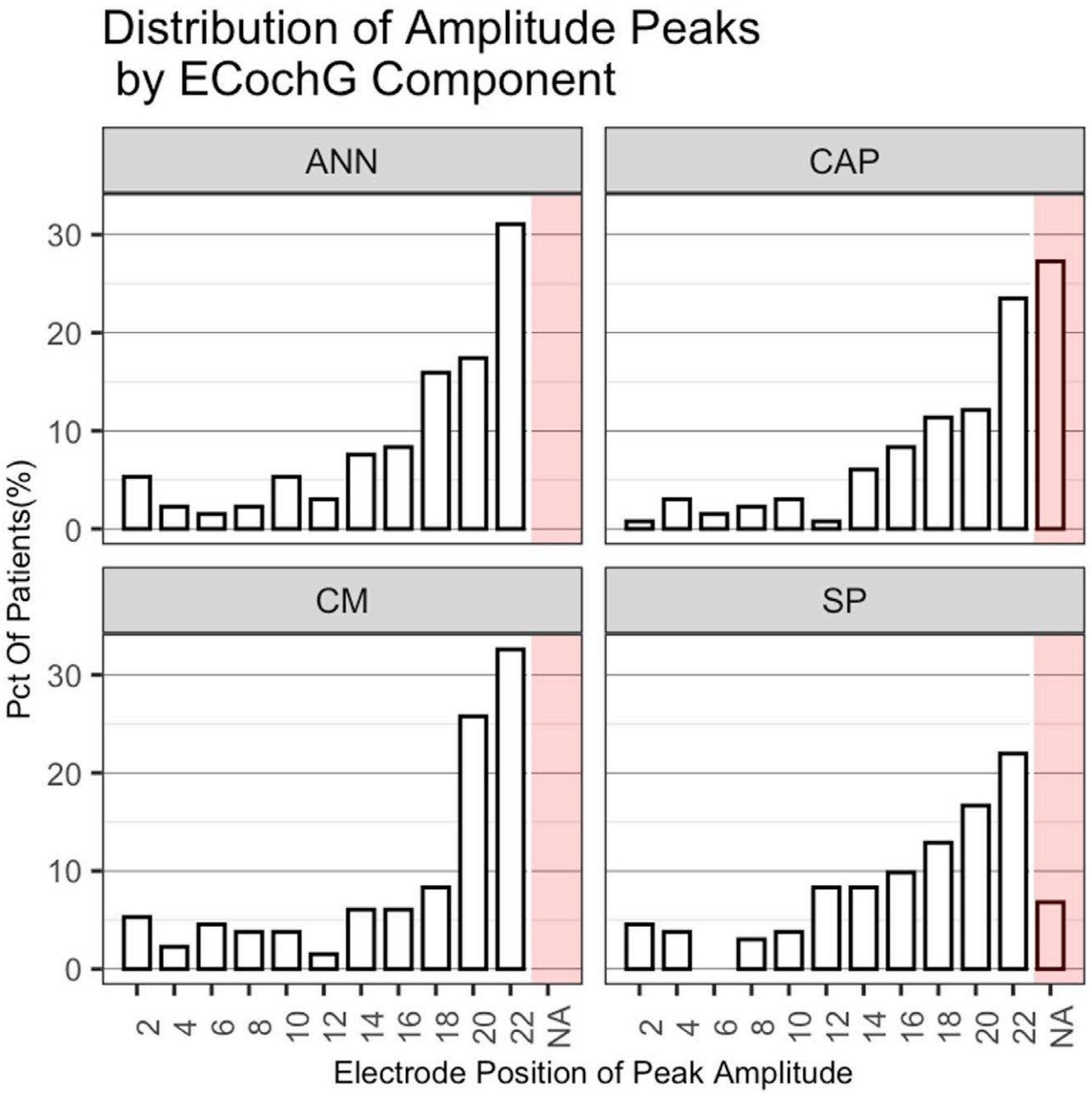

Fig. 5. Distribution of amplitude peaks by electrocochleography (ECochG) component from recording across the whole implant array on every other electrode, from two (most basal recording) to electrode 22 (most apical recording). The red NA section indicates the percentage of patients who did not have the relevant ECochG component detectable (i.e., 0 μV across the array). ANN indicates auditory nerve neurophonic; CAP, compound action potential; CM, cochlear microphonic; SP, summating potential; NA, not applicable.

CM amplitude observed (the peak CM position) was plotted against that of the ANN. There was little change in the value of linear coefficients for these relationships. However, the variance explained, measured as r^2, was notably higher in +SP patients for most relationships (Table 4), aside from the relationship between peak CM and SP electrode locations, where −SP had greater variance explanation (r^2 of −SP 49.4%, +SP 29.6%).

To further SP deflection assessment and its change across the electrode array, responders with large dynamic SP deflection were plotted individually, divided by SP group and ordered by position of peak response from basal to apical electrodes (Figs. 11A–V). There was a wide range of whole-array SP deflection patterns seen. It appeared that recordings with more apically positioned peaks in the +SP group had a similar pattern of change (Figs. 11P–V), showing smaller amplitude negative deflection at the basal region, becoming strongly positively deflected in the apical third of electrodes. The dynamic −SP recordings had less consistent patterns (Figs. 11A–K), as did those patients with more basally positioned +SP peaks. There was no apparent difference between dynamic and unipolar SP responses for their peak electrode response site, median response site remaining the same.

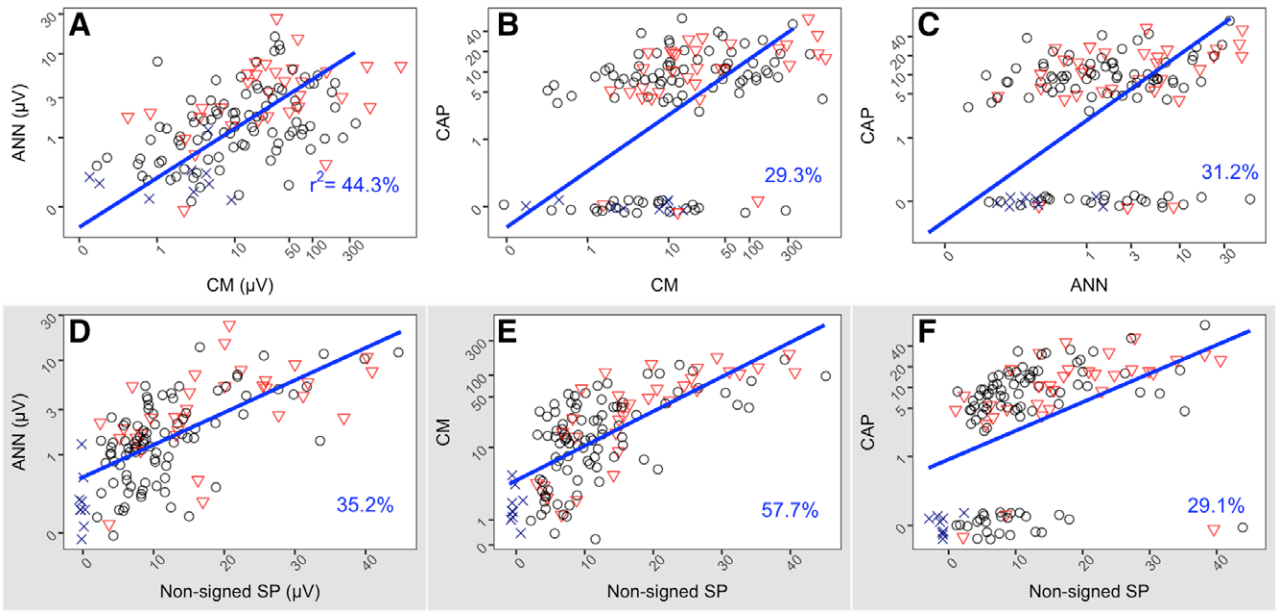

Fig. 6. Plots of maximum amplitudes of electrocochleography (ECochG) components against each other. A–C, have linear best-fit models applied. D–F, (shaded grey) have the same linear models applied to the absolute (nonsigned) SP amplitude. Red triangles represent patients with maximum SP amplitude that had positive deflection of any amplitude; black circle represents patients with negative SP deflection; and the navy X represents patients with zero SP deflection recorded across the array. Logarithmic scales are used for CM, ANN, and CAP amplitudes to reduce clustering. Best fit line in blue with associated r^2 in bottom left corner. For CAP graphics (B, C, and F) points along the zero amplitude line had vertical jitter added to better display data. There was no recordable CAP if response < 3 μV. ANN indicates auditory nerve neurophonic; CAP, compound action potential; CM, cochlear microphonic; SP, summating potential.

TABLE 2. ECochG maximum responses by SP group

	SP Groups			All Pts
	Minimal (≤–10 μV)	Negative (–10 to +10 μV)	Positive (≥+10 μV)	
N	43	45	25	113
CM*	11.6 (13.5)	40.1 (39.5)	77.3 (53.4)	33.5 (41.6)
ANN*	1.2 (1.1)	3.6 (3.4)	5.7 (5.6)	2.9 (3.6)
SP*	–3.8 (4.8)	–17.6 (8.7)	24.2 (12.2)	–3.2 (16.6)
CAP*	4.2 (4.7)	14.5 (13.9)	19.0 (13.8)	10.5 (12.1)

**p < 0.005 for primary outcome difference.*
ANN, auditory nerve neurophonic; CAP, compound action potential; CM, cochlear microphonic; ECochG, electrocochleography; SP, summating potential.

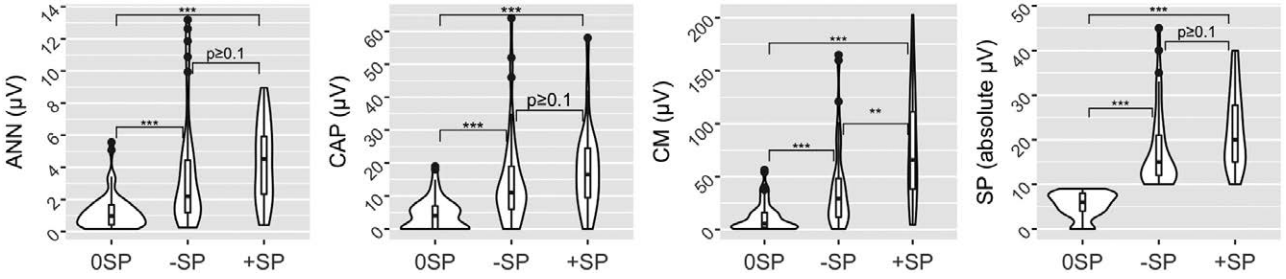

Fig. 7. Violin plot of maximum amplitude of each electrocochleography (ECochG) component by summating potential (SP) grouping. Boxplot with outliers overlaid, margins of box at 25th and 75th centiles, thick bar indicates median point. Brackets show test of differences in groups. ***$p < 0.005$, **$0.005 \le p \le 0.05$, *$0.05 \le p \le 0.1$. SP groups: large negative maximum SP ≤ –10μV (–SP), small or no SP (0 SP), large positive maximum SP ≥ +10μV (+SP). ANN indicates auditory nerve neurophonic; CAP, compound action potential; CM, cochlear microphonic.

SP Group to Preoperative Speech Perception and Audiometric Thresholds. The preoperative audiometric thresholds and CVC-P were affected by the SP grouping (Fig. 12; Kruskal-Wallis sum rank tests p = <0.001 and 0.023, respectively). There were no significant group differences for SRT scores. Pairwise post hoc analysis showed significantly higher CVC-P scores with both +SP than 0 SP responders (p = 0.02) and +SP than −SP responders (p = 0.014). The PTA was higher for 0 SP than +SP (p < 0.001) responders and 0 SP than −SP (p = 0.007) responders.

DISCUSSION

The main finding of this study is that the intracochlear SP, when measured across the whole electrode array, displays

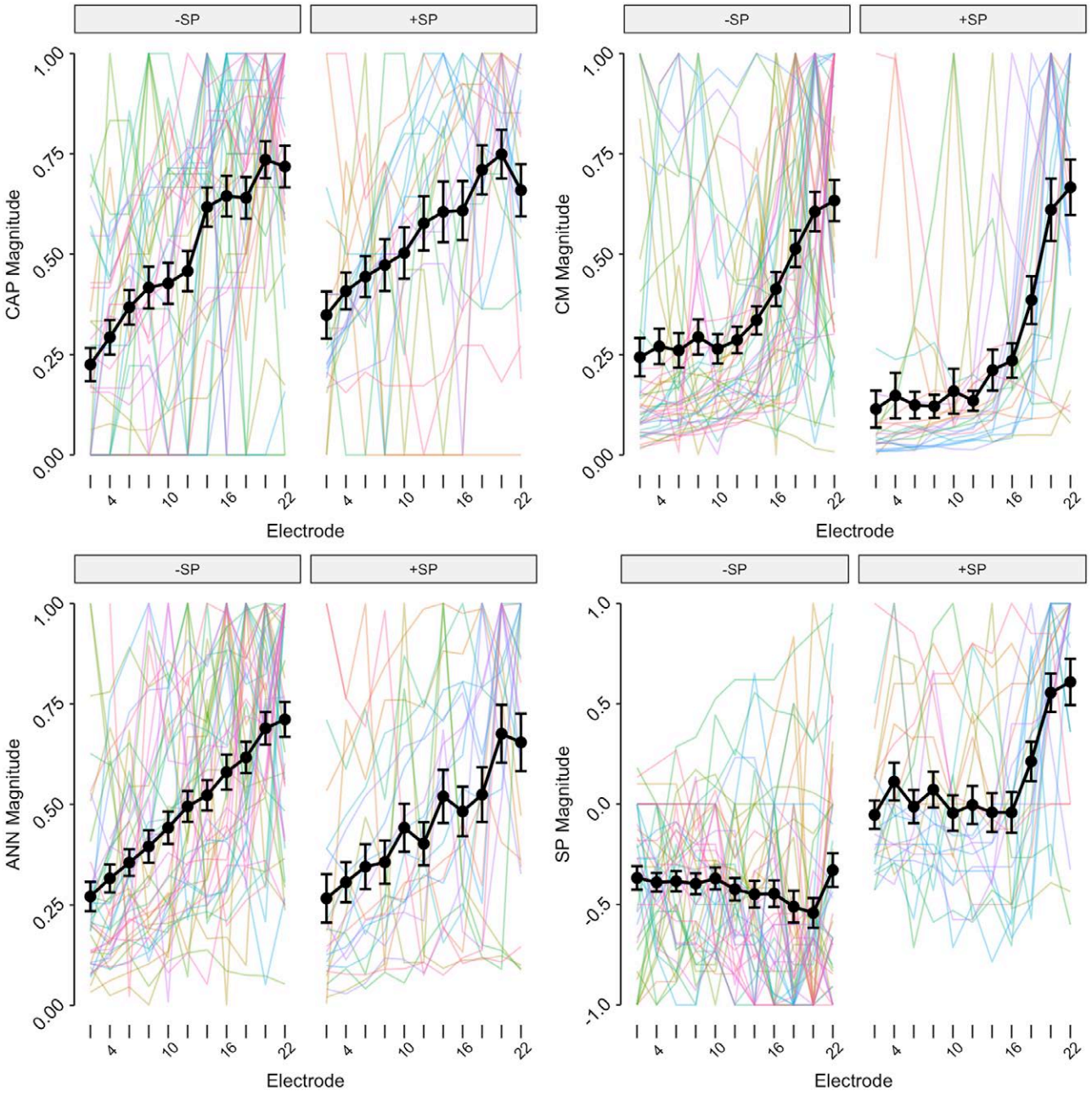

Fig. 8. Patterns of electrocochleography (ECochG) component amplitude growth across the implant array, by summating potential (SP) group. ECochG was recorded in response to a 500-Hz tone burst on every alternate electrode across the array from electrode two (most basal) to 22 (most apical). The color lines are individual patient magnitude plots. The y-axis "Magnitude" scale represents the relative amplitude of the recording at each electrode compared to its peak amplitude. Overlaid in black is the median magnitude at each electrode with interquartile range error bars. SP groups: large negative maximum SP ≤ −10 μV (−SP), large positive maximum SP ≥ +10 μV (+SP). ANN indicates auditory nerve neurophonic; CAP, compound action potential; CM, cochlear microphonic.

unique properties not seen in other ECochG components. Robust SPs were recorded in over half of implant recipients (61.9%) and its maximum deflection in either a positive or negative direction were associated with distinct patterns of ECochG responses and preoperative speech scores. When examined in detail, these patterns suggest that recordings with large positive SPs (+SP) have better preoperative cochlear function than those with large negative SPs (−SP) and minimal to no SP (0 SP). Positive SP deflection may therefore be generated by structure(s) integral to cochlear integrity.

The evidence that SP polarity may provide a unique insight into the cochlear response is as follows. The +SP group had exponential normalized amplitude growth toward the apex to positive deflection. This was distinct from the −SP group that had had smaller apical growth and was generally negatively deflected across the array. These differences in amplitude growth were confirmed by the average amplitudes for each group (+SP mean amplitude @ electrode 22 = +24 μV, @ electrode 2 = +2μV, $p = 0.001$; −SP mean amplitude @ electrode 22 = −12 μV, @ electrode 2 = -7 μV, $p = 0.65$). There was no apparent difference between both groups' growth patterns of ANN, CM,

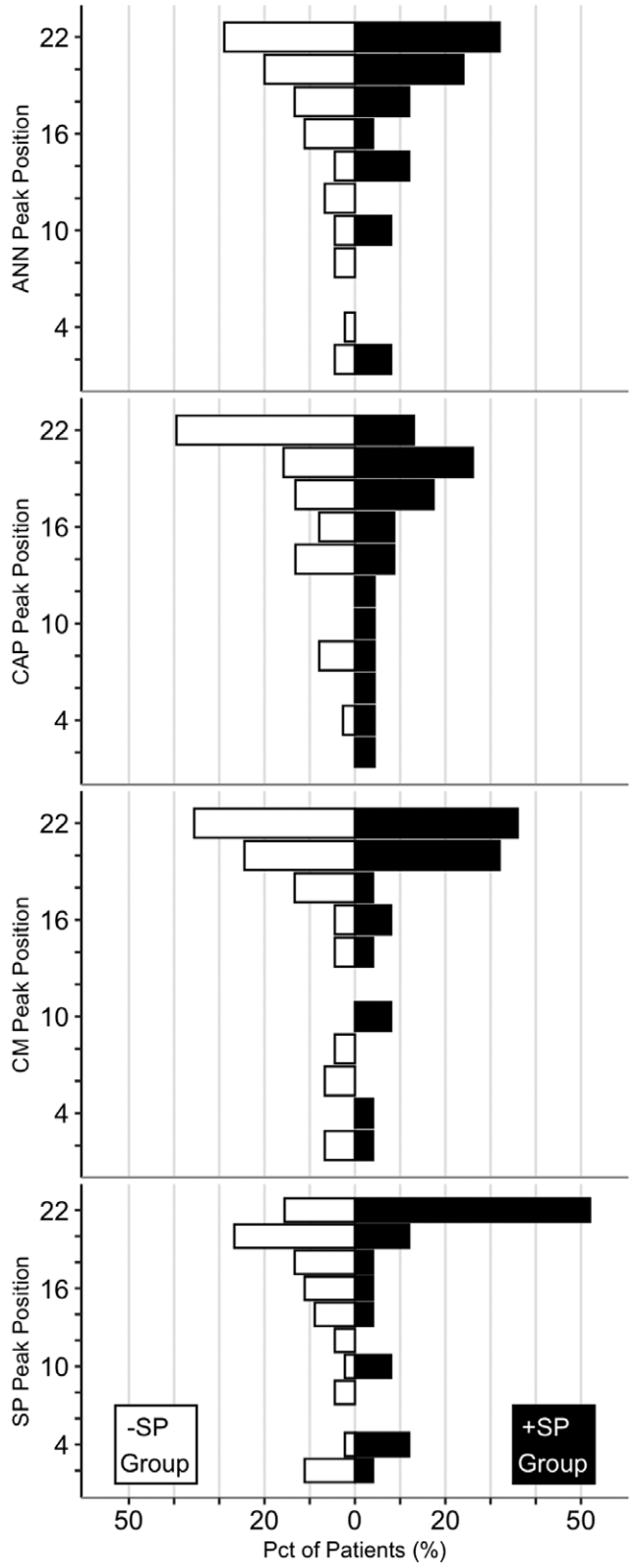

Fig. 9. Distribution of peak electrocochleography (ECochG) responses by summating potential (SP) grouping. SP groups: large negative maximum SP ≤ −10 μV (−SP), large positive maximum SP ≥ +10μV (+SP). ANN indicates auditory nerve neurophonic; CAP, compound action potential; CM, cochlear microphonic.

TABLE 3. Position of maximal electrode location by SP group

	SP Group			All Pts
Waveform n(IQR)	Minimal	Negative	Positive	
N	43	45	25	113
CM	20 (13–22)	20 (14–22)	20 (16–22)	20 (14–22)
ANN	18 (15–22)	18 (12–21)	20 (14–22)	20 (14–22)
SP*		18 (12–20)	22 (14–22)	18 (12–20)
CAP	18 (12–19)	20 (16–22)	18 (13–22)	18 (14–22)

Interquartile ranges in brackets.
**SP electrode comparison only between +SP and −SP groups.*
ANN, auditory nerve neurophonic; CAP, compound action potential; CM, cochlear microphonic; IQR, interquartile range; SP, summating potential.

and CAP (Fig. 8), all showing a growth of amplitude toward the apex. This suggests that these two SP deflection patterns reflect cochlear health differences that are not primarily of OHC or ANF origin, both of which are associated primarily with the CM and ANN, respectively.

Several associations in these data were consistent with the interpretation that functional IHC may be the primary generator of positive IC SP deflection. The first of these is that there was relatively greater spatial specificity of positive SP amplitudes toward the apical electrodes, which are the array electrodes closest to the 500 Hz region of the cochlea (Greenwood 1990). Greater selectivity of SP at the cochleotopic place has been reported previously in animal experiments, and has been attributed to IHC activation at the cochleotopic place (Dallos 1986; Helmstaedter et al. 2018). While we acknowledge that due to the high intensity stimulus used here OHC may also be contributing to the SUM trace deflection due to asymmetric saturation to the input (Pappa et al. 2019), but this does not explain the greater spatial selectivity of the +SP.

Second, preoperative audiometric thresholds and speech perception were different between SP Groups. Both −SP and +SP Groups had lower PTA thresholds prior to implantation compared to the 0 SP, but no significant differences between each other ($p = 0.76$; Fig. 12). These relationships were different for the preoperative speech perception. The +SP group had significantly better phoneme scores compared to the 0 SP and −SP group (preoperative CVC-P for +SP: 46%; 0 SP: 36%; −SP: 34%; $p = 0.018$ and 0.003, respectively). These findings suggest better auditory processing when the +SP pattern was observed, as might be expected with greater IHC function. It must be noted that while these differences are statistically significant, they are modest in size and clinical impact. It is also acknowledged that speech perception is affected by other factors apart from cochlear tissue states including etiology, age, cognition and level of education, which were not controlled for in this study (Heutink et al. 2021; Shechter Shvartzman et al. 2022). No significant differences were seen in the most complex auditory task of speech-in noise (SRT); the lack of difference between groups here might reflect the low ceiling limit of this test.

Cochlear microphonic qualities are also consistent with an association of IHC function to positive SP deflection. Average CM maxima for both groups were large, but the +SP group CM maximum was significantly higher (−SP = 40 μV, +SP = 77 μV, $p = 0.014$). This is despite similar patterns of CM amplitude growth across the array, CM peak positions (both

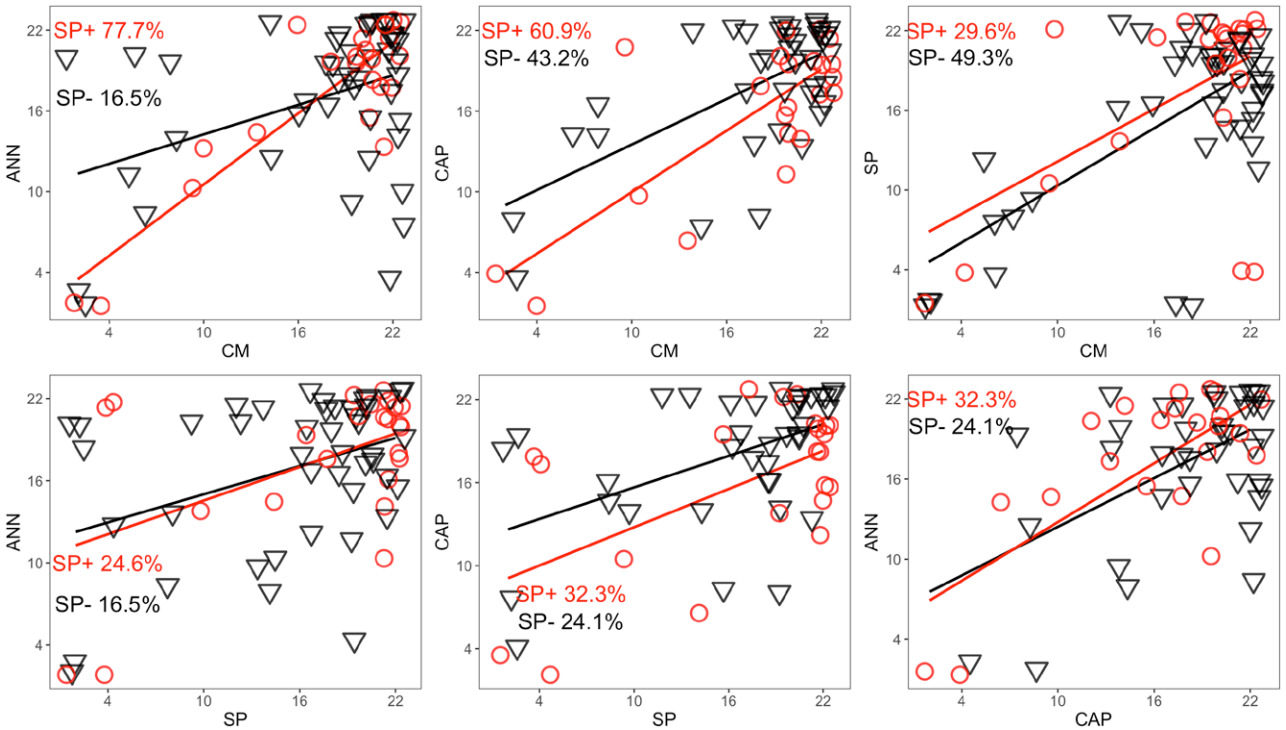

Fig. 10. Plots of electrocochleography (ECochG) component peak positions against one another, by summating potential (SP) group. Red circles are plot points for the positive SP (+SP) group, and black triangles for the negative (−SP) group. Linear model plotted for each group with r^2 noted. ANN indicates auditory nerve neurophonic; CAP, compound action potential; CM, cochlear microphonic.

TABLE 4. Association of different ECochG component peaks across the array, by SP Group

	SP Group		All Pt
Peak:Peak Relationship	Negative	Positive	
CM:ANN	16.5*	77.7†	26.9†
CM:CAP	43.2‡	60.9†	33.5†
CM:SP	49.3†	29.6*	16.7†
SP:CAP	24.1‡	32.3*	15.5†
SP:ANN	16.5§	24.6*	8.2†
ANN:CAP	24.1*	32.3†	20.1†

Adjusted-r^2 values (%) ARE PRESENTED for both −SP and +SP groups, and the whole group ("All Pt").
**p < 0.01;*
†p < 0.001;
‡p ≥ 0.1;
§p < 0.1.
ANN, auditory nerve neurophonic; CAP, compound action potential; CM, cochlear microphonic; ECochG, electrocochleography; SP, summating potential.

groups CM peak at electrode 22) and absolute amplitudes of SP deflection (−SP maximum SP absolute amplitude = 17.6, +SP = 24.2, $p = 0.24$). The moderate to large size of both groups' microphonic indicates that both have a considerable level of hair cell output. We suggest that the significant difference in CM amplitude could be explained by +SP patients having similar OHC levels to −SP patients, but greater IHC numbers that additively contribute to the CM amplitude. The −SP group's overall smaller CM amplitude suggests that two distinct hair cell populations both contribute to CM output, but have opposing contributions to SP deflection. This argument proposes that negative d.c. deflection may be generated the OHC population. When the IHC are present and activated, negative SP deflection is opposed and surmounted by a strong positive deflection.

Conversely, synaptopathy, or a loss of functional IHC with relative maintenance of OHC, could be another proposed underlying mechanism for the relatively better preoperative phoneme scores in the +SP group. Synaptopathy can degrade temporal suprathreshold temporal processing in the cochlea (Liberman & Kujawa 2017). This disproportionately affects speech perception more than audiometry thresholds (Santarelli et al. 2021), so the −SP group may represent patients with fewer neurally-connected IHC than the +SP group, rather than a difference in absolute numbers. Although our focus was not upon etiology-specific SP responses, it is interesting to note that the two confirmed ANSD patients included in this study are within this −SP group, but this number is insufficient to establish any solid conclusions.

Opposing polarity generation of IHC to OHC has been suggested in the literature since SP's infancy. Many have concluded that IHC generate a positive deflection and OHC a negative one (Goldstein 1954; Johnstone & Johnstone 1966; Helmstaedter et al. 2018; Pappa et al. 2019), which is consistent with the findings in our study. However, the inverse has also been described (Davis et al. 1958; Dallos & Cheatham 1976; Rea & Gibson 2003). These contrasting findings may be due to the geometry of the recording electrodes' location relative to the tissue generating ECochG responses.

The effect of differences in geometry must be considered when comparing intra to extracochlear ECochG studies and their findings regarding SP deflection and amplitude. Intracochlear recordings display granularity that is unavailable to extracochlear approaches, with more detail on the apical cochlea and focal tissue responses (Calloway et al. 2014). EC ECochG is

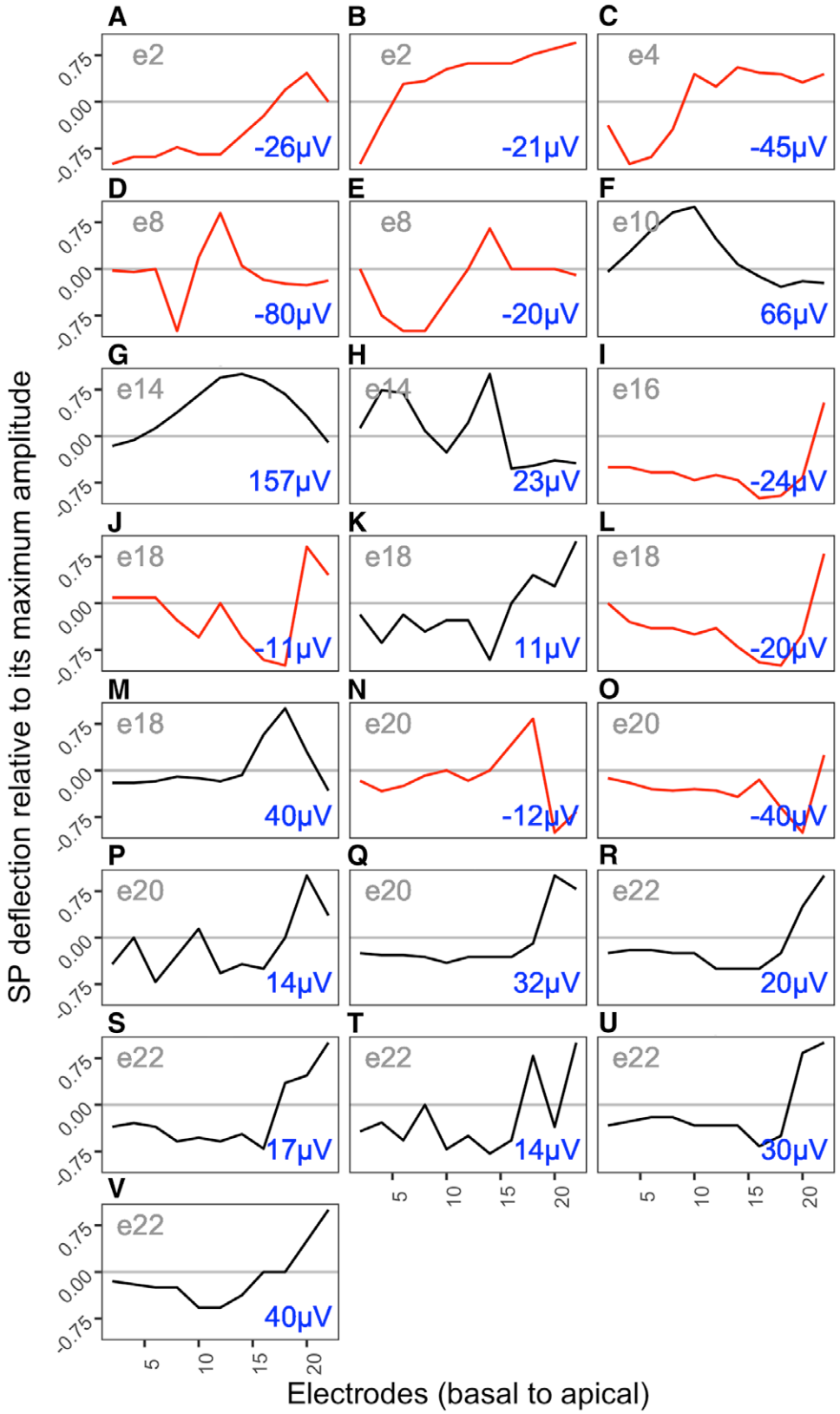

Fig. 11. Patterns of SP deflection in individual patients who had at least one SP amplitude ≥10 μV and at least one other ≤ −10 μV, that is, displaying both large positive and negative SP deflection across the array length. Traces are arranged (A–V) in order of peak SP response electrode position, from most basal (A) and (B) to most apical (R–V). Red plots are in −SP group, black plots indicate +SP group. Number in grey in top left corner indicates the electrode location of peak response. Number in blue in bottom right corner indicates the amplitude and polarity of the peak SP response. SP indicates summating potential.

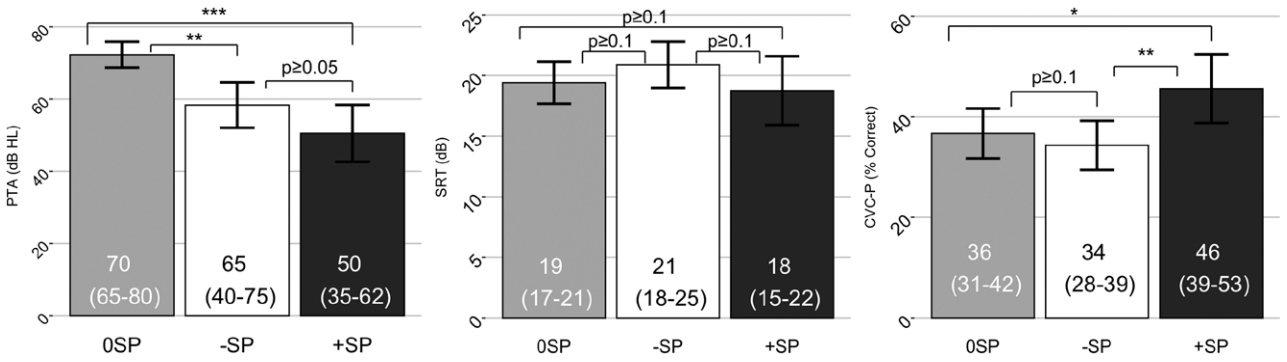

Fig. 12. Preoperative audiometric thresholds and speech perception scores by summating potential (SP) group. SP groups: small or no SP (0 SP), large negative maximum SP ≤ −10 μV (−SP), large positive maximum SP ≥ +10μV (+SP). Mean score in the bar graph with interquartile range in brackets. Tests compared: Pure-tone audiometry average (PTA), speech recognition threshold (SRT), and consonant vowel consonant phoneme (CVC-P) scores. Brackets indicate between-group comparison. *** $p < 0.005$, **$0.005 \leq p \leq 0.05$, *$0.05 \leq p \leq 0.1$.

dominated by the basal turn of the cochlea (Campbell et al. 2010) so it may not be able to detect the focally positive SP deflection in the apical cochlea, as recorded here. Given this is the region of interest for hearing preservation in implantation (Miranda et al. 2014), this added detail is of clinical interest to better understand apical cochlear health and its effect on implant outcome.

In addition, the geometry of the cochlea and the relative position of the recording electrode may affect SP deflection as a separate factor to the underlying tissue characteristics. As shown here and by Helmstaedter et al. (2018), the SP of intracochlear ECochG is dynamic across the length of the array with tonotopicity for positive SP deflection to the characteristic frequency (CF). Therefore, the electrode insertion depth will affect the SP characteristics across the array, especially in its peak position. We attempted to reduce this effect on results by focusing on completely inserted arrays response to a 500 Hz tone, the CF of which is known to be at or more apical to the most apical electrode in fully inserted implant models used in this study (Campbell et al. 2017). Translocation of the array from the scala tympani to the scala media may also invert SP polarity of recordings apical to the site of translocation (Tasaki & Spyropoulos 1959; Koka et al. 2018). While electrode translocation is not seen frequently with the electrode used in this study (Mittmann et al. 2017), postoperative imaging, which was beyond the scope of the present study, would be required to exclude this possibility.

We made one observation consistent with the idea that the laterality of the electrode within scala tympani may affect the SP polarity. Within the dynamic SP responders, the transition point of polarity reversal for SP deflection was most often in the middle third of the electrode array. Here the SP transitioned from a negative to a positive polarity. This transition point is the site where straight electrode arrays move from a relative medial to a lateral position within the cochlear duct (Garaycochea et al. 2020). Given this, we may speculate that laterality could play a role in IC SP deflection in some cases. Again, imaging might provide further insights.

An additional consideration is that the cochleotopic place for a given frequency of simulation trends basally in the cochlea with increasing sensorineural hearing loss (Eggermont 1977). This could push the maximum cochlear response to more basal electrodes on the array than expected form the Greenwood equations.

We observed another relation between ECochG waveforms that may support the IHC generation of positive SP deflection. CM and ANN peak-to-peak correlation was much higher (r^2 = 77.7) for +SP patients compared to −SP (r^2 = 16.5). This could be explained by there being greater numbers of IHC in cochleae exhibiting a positive SP, as these cells are responsible for mechanosensory transduction. We acknowledge that there is overlap of generators to a.c. waveforms when high intensity low frequency are used as in this study, with some contribution of OHC to the a.c. waveform in the SUM trace (Teich et al. 1989), and ANF to the DIF trace (Forgues et al. 2014). So this correlation rise in the +SP group may represent some change in a.c. waveform composition or generation of uncharacteristic harmonics rather than an increase in mechanosensory transduction.

As mentioned earlier, it has been suggested that the CM may be a surrogate marker for overall cochlear health. Several studies have measured an EC ECochG total response (ECochG-TR) in CI recipients and is the current best predictor of postoperative hearing outcomes (Fitzpatrick et al. 2014; McClellan et al. 2014; Formeister et al. 2015; Fontenot et al. 2017, 2019; Giardina et al. 2019; Walia et al. 2022). This ECochG-TR is composed mostly of the CM, with a small ANN contribution. The authors have suggested the effectiveness of ECochG-TR as a predictor is primarily due to its capacity to measure hair cell function, which acts as a surrogate marker of overall cochlear health and underlying neural function. We only found a weak linear correlation between CM maximum and preoperative speech perception (CVC-P r^2 12.8%) and PTA (17%), consistent with previous work showing CM in isolation is an insufficient marker for insertional trauma (Weder et al. 2021). However, in the absence of confirmed synaptopathy, this may suggest that a larger CM at the time of insertion may imply relatively less degraded connection compared to patients with a smaller CM, albeit of small effect. Reduced OHC, IHC, and/or synaptic function have all been associated with degeneration of ANF and their dendrites (Coyat et al. 2019; Ding et al. 2021), but neural degeneration or dysfunction can also occur with normal hair cell responses, as seen in auditory neuropathy (Moser & Starr 2016) and a normal or enlarged CM response can be recorded in cochleae with IHC dysfunction (Santarelli et al. 2009; Shearer & Hansen 2019).

We could not arrive at a single, simple, and coherent explanation for the patterns of large negative SP deflection in our data. The triple generator theory suggests that OHC are the primary

generator of negative EC SP deflection. It therefore is logical to suggest that the primary ECochG response indicating OHC function, the CM, may be associated with negative SP deflection in IC ECochG recordings. There is one point of association between the CM and negative IC SP deflection in our data: the peak-to-peak correlation between CM and SP maxima were the stronger for the −SP Group (r^2 = 49.3), than the +SP group (r^2 = 29.6). However, growth patterns of IC SP and CM amplitude were dissimilar for −SP patients (Fig. 8). This suggests that in CI recipients, the generation of IC negative SP deflection is more complex than OHC function alone. Other possible causes are now discussed.

It may be that these negative deflections are the common end point of multiple different pathological processes, which may not be related. We now briefly consider some potential contributors to negative SP deflection patterns:

1. As outlined earlier, the polarity of the SP depends on the position of the recording electrode relative to its dipole. For both OHC and IHC, the SP is expected to be positive at the center of gravity of its dipole, and negative at locations either side. As proposed by Pappa et al. (2019), the center of gravity of the dipole is expected to be more basal for IHCs than for OHCs, such that a recording electrode can be between the two dipoles, so that one appears positive and the other negative. The IHC center of gravity is more basal because of the greater asymmetry in the IHC operating point, which favors a positive over a negative membrane potential (Johnstone & Johnstone 1966), such that the basal spread of excitation for IHCs is greater than for OHCs. Thus electrode geometry may explain the polarity of the SP; in +SP cases the dipole of either IHCs or both OHCs and IHCs is basal enough to be crossed, while for −SP cases it is not, either because the elements themselves are fewer or the electrode was inserted less deeply.

Consistent with this explanation is the observation that the greatest CM is associated with the greatest positive SP (Table 2), because a larger response suggests a larger population of responding elements supporting a greater spread of excitation. That is, the IHC dipole (at least, may be OHCs as well in some cases) is at a basal enough point where it can be crossed. It is also consistent with a greater proportion of −SPs than +SPs, because the number of cases with enough residual hair cell activity for the dipole to be crossed is relatively small. This explanation does not require the predominance of cases to have greater preservation of OHCs than IHCs, and is potentially more aligned with current understandings of most cochlear pathologies, where greater IHC than OHC survival is expected.

2. A cochlear dead region in the apex. If positive SP deflection is tonotopic to the CF, a lack of functional tissue in the cochlear apex could result in an absence of a positive SP to a 500 Hz tone, leaving only negative SP deflections from more basal cochlear regions (Helmstaedter et al. 2018). Apical hair cells, both IHC and OHC, may produce more d.c. output than their basal counterparts regardless of CF (Wang et al. 2016). In either of these situations, an apical dead region may result in a similar across-array SP pattern. Median CM amplitudes for apical electrodes for −SP groups were smaller than +SP groups (−SP 15 μV, +SP 49 μV), which may support a dead region contribution to the −SP deflection pattern.
3. Trauma or contact between the electrode and the basilar membrane. This may impair the propagation of the travelling wave along the BM and thereby reduce cochlear output at sites more apical to this trauma or interaction (Campbell et al. 2016; Giardina et al. 2019). Pressure on the BM can also reverse the polarity of the SP at the site of interaction (Johnstone & Johnstone 1966). ECochG changes in response to implant-BM interaction during CI insertion are well documented (Kim 2020), but the relationship between postinsertional IC SP deflection and trauma is not well described in humans. Postoperative imaging can detect translocation and scalar trauma with some accuracy (Riggs et al. 2019; Liebscher et al. 2020), which was not utilized in this study. Correlation of the IC SP to imaging in future studies may illuminate this relationship further.
4. Neural tissue contribution. Parts of SP deflections have been attributed to isolated asynchronous action potentials of various nerve fibers (Kupperman 1966). Generally, these have been observed as small to medium negative deflections (Dallos & Cheatham 1976; Zheng et al. 1997; Kennedy et al. 2017), although Pappa et al. found neural tissue produced a very small ongoing positive deflection of the SP (Pappa et al. 2019). It is difficult to reconcile these contrasting findings. In our study, neither CAP nor ANN had significant amplitude or peak position associations in either negative or positive SP groups. Riggs et al. (2017) visually examined extracochlear ANN and CAP in CI recipients, measured as a nerve score, and found ANSD and non-ANSD groups' scores were similar. This suggests that in CI recipients, simple analysis of these neural ECochG components may not accurately reflect underlying neural tissue function. If this is the case, the neural contribution to the SP may not be related to ANN or CAP amplitude in a straightforward manner. In addition, if the neural contribution to the SP is small, its effect may be masked by larger-amplitude contributors to SP deflection.
5. Artefact contribution to negative drift of ECochG recordings. A slight negative drift of the recording baseline was observed in many cases. We cannot exclude the possibility that our ECochG recordings had a negative deflection d.c. artefact. which may have made recordings with minimal SP deflection skew toward the negative.

This study had limited data on the etiology of hearing loss, with the majority of patients having and unknown cause. Genetic causes of hearing impairment and ANSD both can have an effect on SP deflection (Santarelli et al. 2013, 2015). Future examination of IC ECochG with more genomic or etiological data would illuminate SP deflection in a clearer light.

Some studies have associated large positive SPs with pathological processes. An abnormal positive potential (APP), a large positive d.c. deflection in the absence of a CAP, has been described in tone-stimulus RW ECochG performed on neonates and infants with severe to profound hearing loss (O'Leary et al. 2000; Rea & Gibson 2003). Rea and Gibson (2003) speculated that the APP was generated by OHC activity with relative IHC loss (Rea & Gibson 2003), although the evidence was somewhat

circumstantial. O'Leary et al. (2000) put forward a different theory that the APP is generated by active hair cells in the cochlear base in the absence of neural activity. A more recent study by Grant et al. (2020) of RW ECochG investigated click-evoked SPs. They found these SPs were larger and CAPs smaller in those with poorer hearing-in-noise performance, suggesting that cochlear neural deficits contributed to the SP changes.

On the surface, these studies contrast with our finding that large positive SPs had superior preoperative audiometry and speech perception. We did not find that SP deflection was correlated with either CAP or ANN patterns, which did not support the theory of deficient neural tissue causing positive deflection. Regarding the basal region origin of positive SP deflection, we did not find that positive SP deflection was associated with basal cochlear hair cell activity. There are several possible explanations for these contrasting findings including the differences in geometry as mentioned above.

Other possible contributing factors are as follows:

1. The difference in patient groups studied, especially for the normal-hearing study compared to our CI recipients. We therefore cannot exclude the possibility that a large positive IC SP is pathological in nature. However, it appears that it is related to a cochlear state that causes less auditory processing impairment than pathologies that cause a negative IC SP or no deflection.
2. Responses of click- to tone-evoked SPs are dissimilar (Iseli & Gibson 2010) making the findings of Grant et al. (2020) not directly relatable to ours.
3. The difference in tonal stimulus parameters between studies. O'Leary et al. (2000) did not find any APP to a 500 Hz tone, and Rea and Gibson (2003) did not mention which stimulus tones elicited an APP. This final point may indicate that our method may not be suitable to detect an APP, if it is measurable from an IC approach.

It is interesting to note that CAP amplitude showed a similar growth pattern toward the apex similar to other ECochG components. This is despite CAP being considered a far-field ECochG component that is thought to derive predominantly from the auditory nerve entering the dura near or within the internal auditory meatus (Brown & Patuzzi 2010). Therefore, the apical skew of CAP maxima seen here may be unrelated to the similar patterns seen in the known near-field generated IC ECochG components. One explanation for this seeming association may be that by virtue of IC electrode geometry relative to the internal auditory meatus, the CAP may have similar peak positioning toward the apex regardless of the stimulus used. Due to the single-tone stimulus used in this study, we were unable to differentiate tone-specific IC CAP qualities. It may also be true that there is a component of the CAP that is near-field generated, contrary to our current understanding of its generation. In CI recipients, CAPs are often absent, and if present are usually small and of highly variable morphology (Scott et al. 2016), so its utility for neural tissue interrogation, like the ANN, may not be reliable or useful clinically (Riggs et al. 2017).

CONCLUSIONS

The summating potential can be recorded in CI recipients from an intracochlear approach across the electrode array. It displays cross-array qualities that show it is distinct from the CM, CAP, and ANN. Patients with large positive SPs had lower auditory thresholds and higher preoperative phoneme scores than patients with minimal SP or a predominantly negative SP. While definitive conclusions cannot be reached, associations in these data suggest that the positive SP could reflect greater residual hair cell activity, potentially IHC function, in these patients. As such, the positive SP may reflect ears with better cochlear health. The data did not suggest a definitive explanation for negative SP deflection. These results will further inform our understanding of implant function and the underlying pathology contributing to deafness.

ACKNOWLEDGMENTS

We would like to thank engineers from Cochlear Ltd. for assistance in developing software, the audiologists and staff at the Royal Victorian Eye and Ear Hospital Implant Clinic for their support during the project, and the surgeons and surgical registrars of the clinic.

Acquisition of the data was supported by Cochlear Ltd. J. P. was funded by an Australian Commonwealth Government scholarship. S. L. was funded by the National Health and Medical Research Council (Australia), GNT0628679 and GNT107867.

J.P. wrote this manuscript alone, with proofreading done by C.B. and S.O. MATLAB coding was mainly performed by C.B. Statistical analysis was performed by J.P. with guidance by the Statistical Consulting Platform of the University of Melbourne.

The authors have no conflicts of interest to disclose.

Address for correspondence: Stephen O'Leary, Royal Victorian Eye and Ear Hospital, 32 Gisborne Street, Melbourne, Victoria, Australia. E-mail: sjoleary@unimelb.edu.au

Received January 13, 2022; accepted January 13, 2023; published online ahead of print March 20, 2023.

REFERENCES

Adunka, O., Roush, P., Grose, J., Macpherson, C., Buchman, C. A. (2006). Monitoring of cochlear function during cochlear implantation. *Laryngoscope*, *116*, 1017–1020.

Bench, J., Kowal, A., Bamford, J. (1979). The BKB (Bamford-Kowal-Bench) sentence lists for partially-hearing children. *Br J Audiol*, *13*, 108–112.

Bester, C., Dalbert, A., Collins, A., Razmovski, T., Gerard, J. M., & O'Leary, S. (2022, Dec 23). Electrocochleographic Patterns Predicting Increased Impedances and Hearing Loss after Cochlear Implantation. *Ear Hear.* https://doi.org/10.1097/AUD.0000000000001319.

Bester, C. W., Campbell, L., Dragovic, A., Collins, A., O'Leary, S. J. (2017). Characterizing electrocochleography in cochlear implant recipients with residual low-frequency hearing. *Front Neurosci*, *11*, 141.

Blamey, P., Artieres, F., Baskent, D., et al.. (2013). Factors affecting auditory performance of postlinguistically deaf adults using cochlear implants: An update with 2251 patients. *Audiol Neurootol*, *18*, 36–47.

Bland, J. M., & Altman, D. G. (1986). Statistical methods for assessing agreement between two methods of clinical measurement. *Lancet*, *1*, 307–310. https://www.ncbi.nlm.nih.gov/pubmed/2868172.

Brown, D. J., & Patuzzi, R. B. (2010). Evidence that the compound action potential (CAP) from the auditory nerve is a stationary potential generated across dura mater. *Hear Res*, *267*, 12–26.

Calloway, N. H., Fitzpatrick, D. C., Campbell, A. P., Iseli, C., Pulver, S., Buchman, C. A., Adunka, O. F. (2014). Intracochlear electrocochleography during cochlear implantation. *Otol Neurotol*, *35*, 1451–1457.

Campbell, A. P., Suberman, T. A., Buchman, C. A., Fitzpatrick, D. C., Adunka, O. F. (2010). Correlation of early auditory potentials and intracochlear electrode insertion properties: An animal model featuring near real-time monitoring. *Otol Neurotol*, *31*, 1391–1398.

Campbell, L., Kaicer, A., Briggs, R., O'Leary, S. (2015). Cochlear response telemetry: Intracochlear electrocochleography via cochlear implant neural response telemetry pilot study results. *Otol Neurotol*, *36*, 399–405.

Campbell, L., Kaicer, A., Sly, D., Iseli, C., Wei, B., Briggs, R., O'Leary, S. (2016). Intraoperative real-time cochlear response telemetry predicts hearing preservation in cochlear implantation. *Otol Neurotol*, *37*, 332–338.

Campbell, L., Bester, C., Iseli, C., Sly, D., Dragovic, A., Gummer, A. W., O'Leary, S. (2017). Electrophysiological evidence of the basilar-membrane travelling wave and frequency place coding of sound in cochlear implant recipients. *Audiol Neurootol*, *22*, 180–189.

Coyat, C., Cazevieille, C., Baudoux, V., Larroze-Chicot, P., Caumes, B., Gonzalez-Gonzalez, S. (2019). Morphological consequences of acoustic trauma on cochlear hair cells and the auditory nerve. *Int J Neurosci*, *129*, 580–587.

Dalbert, A., Pfiffner, F., Roosli, C., Thoele, K., Sim, J. H., Gerig, R., Huber, A. M. (2015). Extra- and intracochlear electrocochleography in cochlear implant recipients. *Audiol Neurootol*, *20*, 339–348.

Dallos, P. (1972). Cochlear potentials. A status report. *Audiology*, *11*, 29–41.

Dallos, P. (1986). Neurobiology of cochlear inner and outer hair cells: Intracellular recordings. *Hear Res*, *22*, 185–198.

Dallos, P., & Cheatham, M. A. (1976). Production of cochlear potentials by inner and outer hair cells. *J Acoust Soc Am*, *60*, 510–512.

Davis, H., Deatherage, B. H., Eldredge, D. H., Smith, C. A. (1958). Summating potentials of the cochlea. *Am J Physiol*, *195*, 251–261.

Ding, D., Jiang, H., Salvi, R. (2021). Cochlear spiral ganglion neuron degeneration following cyclodextrin-induced hearing loss. *Hear Res*, *400*, 108125.

Eggermont, J. J. (1976). Analysis of compound action potential responses to tone bursts in the human and guinea pig cochlea. *J Acoust Soc Am*, *60*, 1132–1139.

Eggermont, J. J. (1977). Compound actionpotential tuning curves in normal and pathological human ears. *J Acoust Soc Am*, *62*, 1247–1251.

Ferraro, J. A., Thedinger, B. S., Mediavilla, S. J., Blackwell, W. L. (1994). Human summating potential to tone bursts: Observations on tympanic membrane versus promontory recordings in the same patients. *J Am Acad Audiol*, *5*, 24–29. https://www.ncbi.nlm.nih.gov/pubmed/8155891.

Fitzpatrick, D. C., Campbell, A. P., Choudhury, B., Dillon, M. T., Forgues, M., Buchman, C. A., Adunka, O. F. (2014). Round window electrocochleography just before cochlear implantation: Relationship to word recognition outcomes in adults. *Otol Neurotol*, *35*, 64–71.

Fontenot, T. E., Giardina, C. K., Teagle, H. F., Park, L. R., Adunka, O. F., Buchman, C. A., Brown, K. D., Fitzpatrick, D. C. (2017). Clinical role of electrocochleography in children with auditory neuropathy spectrum disorder. *Int J Pediatr Otorhinolaryngol*, *99*, 120–127.

Fontenot, T. E., Giardina, C. K., Dillon, M., Rooth, M. A., Teagle, H. F., Park, L. R., Brown, K. D., Adunka, O. F., Buchman, C. A., Pillsbury, H. C., Fitzpatrick, D. C. (2019). Residual cochlear function in adults and children receiving cochlear implants: Correlations with speech perception outcomes. *Ear Hear*, *40*, 577–591.

Forgues, M., Koehn, H. A., Dunnon, A. K., Pulver, S. H., Buchman, C. A., Adunka, O. F., Fitzpatrick, D. C. (2014). Distinguishing hair cell from neural potentials recorded at the round window. *J Neurophysiol*, *111*, 580–593.

Formeister, E. J., McClellan, J. H., Merwin, W. H. 3rd, Iseli, C. E., Calloway, N. H., Teagle, H. F., Buchman, C. A., Adunka, O. F., Fitzpatrick, D. C. (2015). Intraoperative round window electrocochleography and speech perception outcomes in pediatric cochlear implant recipients. *Ear Hear*, *36*, 249–260.

Garaycochea, O., Manrique-Huarte, R., Lazaro, C., Huarte, A., Prieto, C., Alvarez de Linera-Alperi, M., Manrique, M. (2020). Comparative study of two different perimodiolar and a straight cochlear implant electrode array: Surgical and audiological outcomes. *Eur Arch Otorhinolaryngol*, *277*, 69–76.

Giardina, C. K., Brown, K. D., Adunka, O. F., Buchman, C. A., Hutson, K. A., Pillsbury, H. C., Fitzpatrick, D. C. (2019). Intracochlear electrocochleography: Response patterns during cochlear implantation and hearing preservation. *Ear Hear*, *40*, 833–848.

Goldstein, R. (1954). Analysis of summating potential in cochlear responses of guinea pigs. *Am J Physiol*, *178*, 331–337.

Grant, K. J., Mepani, A. M., Wu, P., Hancock, K. E., de Gruttola, V., Liberman, M. C., Maison, S. F. (2020). Electrophysiological markers of cochlear function correlate with hearing-in-noise performance among audiometrically normal subjects. *J Neurophysiol*, *124*, 418–431.

Greenwood, D. D. (1990). A cochlear frequency-position function for several species--29 years later. *J Acoust Soc Am*, *87*, 2592–2605.

Hancock, K. E., O'Brien, B., Santarelli, R., Liberman, M. C., Maison, S. F. (2021). The summating potential in human electrocochleography: Gaussian models and Fourier analysis. *J Acoust Soc Am*, *150*, 2492.

Harvey, D., & Steel, K. P. (1992). The development and interpretation of the summating potential response. *Hear Res*, *61*, 137–146.

Helmstaedter, V., Lenarz, T., Erfurt, P., Kral, A., Baumhoff, P. (2018). The summating potential is a reliable marker of electrode position in electrocochleography: Cochlear implant as a theragnostic probe. *Ear Hear*, *39*, 687–700.

Heutink, F., Verbist, B. M., van der Woude, W. J., Meulman, T. J., Briaire, J. J., Frijns, J. H. M., Vart, P., Mylanus, E. A. M., Huinck, W. J. (2021). Factors influencing speech perception in adults with a cochlear implant. *Ear Hear*, *42*, 949–960.

Iseli, C., & Gibson, W. (2010). A comparison of three methods of using transtympanic electrocochleography for the diagnosis of Meniere's disease: Click summating potential measurements, tone burst summating potential amplitude measurements, and biasing of the summating potential using a low frequency tone. *Acta Otolaryngol*, *130*, 95–101.

Johnstone, J. R., & Johnstone, B. M. (1966). Origin of summating potential. *J Acoust Soc Am*, *40*, 1405–1413.

Kennedy, A. E., Kaf, W. A., Ferraro, J. A., Delgado, R. E., Lichtenhan, J. T. (2017). Human summating potential using continuous loop averaging deconvolution: Response amplitudes vary with tone burst repetition rate and duration. *Front Neurosci*, *11*, 429.

Kim, J. S. (2020). Electrocochleography in cochlear implant users with residual acoustic hearing: A systematic review. *Int J Environ Res Public Health*, *17*, 7043.

Koka, K., Saoji, A. A., Litvak, L. M. (2017). Electrocochleography in cochlear implant recipients with residual hearing: Comparison with audiometric thresholds. *Ear Hear*, *38*, e161–e167.

Koka, K., Riggs, W. J., Dwyer, R., Holder, J. T., Noble, J. H., Dawant, B. M., Ortmann, A., Valenzuela, C. V., Mattingly, J. K., Harris, M. M., O'Connell, B. P., Litvak, L. M., Adunka, O. F., Buchman, C. A., Labadie, R. F. (2018). Intra-cochlear electrocochleography during cochear implant electrode insertion is predictive of final scalar location. *Otol Neurotol*, *39*, e654–e659.

Kupperman, R. (1966). The dynamic DC potential in the cochlea of the guinea pig (summating potential). *Acta Otolaryngol*, *62*, 465–480.

Liberman, M. C., & Kujawa, S. G. (2017). Cochlear synaptopathy in acquired sensorineural hearing loss: Manifestations and mechanisms. *Hear Res*, *349*, 138–147.

Liebscher, T., Mewes, A., Hoppe, U., Hornung, J., Brademann, G., Hey, M. (2020). Electrode translocations in perimodiolar cochlear implant electrodes: Audiological and electrophysiological outcome. *Z Med Phys*, *31*:265–275.

McClellan, J. H., Formeister, E. J., Merwin, W. H. 3rd, Dillon, M. T., Calloway, N., Iseli, C., Buchman, C. A., Fitzpatrick, D. C., Adunka, O. F. (2014). Round window electrocochleography and speech perception outcomes in adult cochlear implant subjects: Comparison with audiometric and biographical information. *Otol Neurotol*, *35*, e245–e252.

Miranda, P. C., Sampaio, A. L., Lopes, R. A., Ramos Venosa, A., de Oliveira, C. A. (2014). Hearing preservation in cochlear implant surgery. *Int J Otolaryngol*, *2014*, 468515.

Mittmann, P., Todt, I., Ernst, A., Rademacher, G., Mutze, S., Goricke, S., Schlamann, M., Lang, S., Arweiler-Harbeck, D., Christov, F. (2017). Radiological and NRT-ratio-based estimation of slim straight cochlear implant electrode positions: A multicenter study. *Ann Otol Rhinol Laryngol*, *126*, 73–78.

Moser, T., & Starr, A. (2016). Auditory neuropathy--neural and synaptic mechanisms. *Nat Rev Neurol*, *12*, 135–149.

O'Leary, S., Briggs, R., Gerard, J. M., Iseli, C., Wei, B. P. C., Tari, S., Rousset, A., Bester, C. (2020). Intraoperative Observational Real-time Electrocochleography as a Predictor of Hearing Loss After Cochlear Implantation: 3 and 12 Month Outcomes. *Otol Neurotol, 41,* 1222–1229. https://doi.org/10.1097/MAO.0000000000002773.

O'Leary, S. J., Mitchell, T. E., Gibson, W. P., Sanli, H. (2000). Abnormal positive potentials in round window electrocochleography. *Am J Otol*, *21*, 813–818. https://www.ncbi.nlm.nih.gov/pubmed/11078069.

Pappa, A. K., Hutson, K. A., Scott, W. C., Wilson, J. D., Fox, K. E., Masood, M. M., Giardina, C. K., Pulver, S. H., Grana, G. D., Askew, C., Fitzpatrick, D. C. (2019). Hair cell and neural contributions to the cochlear summating potential. *J Neurophysiol*, *121*, 2163–2180.

Peterson, G. E., & Lehiste, I. (1962). Revised CNC lists for auditory tests. *J Speech Hear Disord*, *27*, 62–70.

Rea, P. A., & Gibson, W. P. (2003). Evidence for surviving outer hair cell function in congenitally deaf ears. *Laryngoscope*, *113*, 2030–2034.

Riggs, W. J., Roche, J. P., Giardina, C. K., Harris, M. S., Bastian, Z. J., Fontenot, T. E., Buchman, C. A., Brown, K. D., Adunka, O. F., Fitzpatrick, D. C. (2017). Intraoperative electrocochleographic characteristics of auditory neuropathy spectrum disorder in cochlear implant subjects. *Front Neurosci*, *11*, 416.

Riggs, W. J., Dwyer, R. T., Holder, J. T., Mattingly, J. K., Ortmann, A., Noble, J. H., Dawant, B. M., Valenzuela, C. V., O'Connell, B. P., Harris, M. S., Litvak, L. M., Koka, K., Buchman, C. A., Labadie, R. F., Adunka, O. F. (2019). Intracochlear electrocochleography: Influence of scalar position of the cochlear implant electrode on postinsertion results. *Otol Neurotol*, *40*, e503–e510.

Santarelli, R., Del Castillo, I., Rodriguez-Ballesteros, M., Scimemi, P., Cama, E., Arslan, E., Starr, A. (2009). Abnormal cochlear potentials from deaf patients with mutations in the otoferlin gene. *J Assoc Res Otolaryngol*, *10*, 545–556.

Santarelli, R., del Castillo, I., Starr, A. (2013). Auditory neuropathies and electrocochleography. *Hear Balance Commun*, *11*, 130–137.

Santarelli, R., del Castillo, I., Cama, E., Scimemi, P., Starr, A. (2015). Audibility, speech perception and processing of temporal cues in ribbon synaptic disorders due to OTOF mutations. *Hear Res*, *330*(Pt B), 200–212.

Santarelli, R., Scimemi, P., Costantini, M., Dominguez-Ruiz, M., Rodriguez-Ballesteros, M., Del Castillo, I. (2021). Cochlear synaptopathy due to mutations in OTOF gene may result in stable mild hearing loss and severe impairment of speech perception. *Ear Hear 42*, 1627–1639.

Scott, W. C., Giardina, C. K., Pappa, A. K., Fontenot, T. E., Anderson, M. L., Dillon, M. T., Brown, K. D., Pillsbury, H. C., Adunka, O. F., Buchman, C. A., Fitzpatrick, D. C. (2016). The compound action potential in subjects receiving a cochlear implant. *Otol Neurotol*, *37*, 1654–1661.

Shearer, A. E., & Hansen, M. R. (2019). Auditory synaptopathy, auditory neuropathy, and cochlear implantation. *Laryngoscope Investig Otolaryngol*, *4*, 429–440.

Shearer, A. E., Tejani, V. D., Brown, C. J., Abbas, P. J., Hansen, M. R., Gantz, B. J., Smith, R. J. H. (2018). In vivo electrocochleography in hybrid cochlear implant users implicates TMPRSS3 in spiral ganglion function. *Sci Rep*, *8*, 14165.

Shechter Shvartzman, L., Lavie, L., Banai, K. (2022). Speech perception in older adults: An interplay of hearing, cognition, and learning? *Front Psychol*, *13*, 816864.

Sijgers, L., Pfiffner, F., Grosse, J., Dillier, N., Koka, K., Roosli, C., Huber, A., Dalbert, A. (2021). Simultaneous intra- and extracochlear electrocochleography during cochlear implantation to enhance response interpretation. *Trends Hear*, *25*, 2331216521990594.

Snyder, R. L., & Schreiner, C. E. (1984). The auditory neurophonic: Basic properties. *Hear Res*, *15*, 261–280.

Tasaki, I., & Spyropoulos, C. S. (1959). Stria vascularis as source of endocochlear potential. *J Neurophysiol*, *22*, 149–155.

Teich, M. C., Khanna, S. M., Keilson, S. E. (1989). Nonlinear dynamics of cellular vibrations in the organ of Corti. *Acta Otolaryngol Suppl*, *467*, 265–279.

Trecca, E. M. C., Riggs, W. J., Mattingly, J. K., Hiss, M. M., Cassano, M., Adunka, O. F. (2020). Electrocochleography and cochlear implantation: A systematic review. *Otol Neurotol*, *41*, 864–878.

Walia, A., Shew, M. A., Kallogjeri, D., Wick, C. C., Durakovic, N., Lefler, S. M., Ortmann, A. J., Herzog, J. A., Buchman, C. A. (2022). Electrocochleography and cognition are important predictors of speech perception outcomes in noise for cochlear implant recipients. *Sci Rep*, *12*, 3083.

Wang, D., Xiong, B., Xiong, F., Chen, G. D., Hu, B. H., Sun, W. (2016). Apical hair cell degeneration causes the increase in the amplitude of summating potential. *Acta Otolaryngol*, *136*, 1255–1260.

Weder, S., Bester, C., Collins, A., Shaul, C., Briggs, R. J., O'Leary, S. (2021). Real time monitoring during cochlear implantation: Increasing the accuracy of predicting residual hearing outcomes. *Otol Neurotol*, *42*, e1030–e1036.

Zhan, K. Y., Adunka, O. F., Eshraghi, A., Riggs, W. J., Prentiss, S. M., Yan, D., Telischi, F. F., Liu, X., He, S. (2021). Electrophysiology and genetic testing in the precision medicine of congenital deafness: A review. *J Otol*, *16*, 40–46.

Zheng, X. -Y., Ding, D. -L., McFadden, S. L., Henderson, D. (1997). Evidence that inner hair cells are the major source of cochlear summating potentials. *Hear Res*, *113*, 76–88.